

(NASA-CR-145144) BEARINGLESS HELICOPTER
MAIN ROTOR DEVELOPMENT. VOLUME 2: COMBINED
LOAD FATIGUE EVALUATION OF WEATHERED
GRAPHITE/EPOXY COMPOSITE Final Report, May
1975 - Dec. 1981 Sikorsky Aircraft, Stratford, G3/24 25129
N77-22177
HC A03/MF A01
Unclass

NASA CR-145144 Volume II
SER-70238

BEARINGLESS HELICOPTER MAIN ROTOR DEVELOPMENT*

Volume II

Combined Load Fatigue Evaluation of Weathered
Graphite/Epoxy Composite

by

Joseph J. Rackiewicz

* The contract research effort which has lead to the results in
this report was financially supported by USAAMRDL (Langley
Directorate).

Prepared Under Contract NAS1-13882

by

Sikorsky Aircraft Division
United Technologies Corporation
Stratford, Conn.

for

NASA
National Aeronautics and
Space Administration

REPORT DOCUMENTATION PAGE		READ INSTRUCTIONS BEFORE COMPLETING FORM
1. REPORT NUMBER	2. GOVT ACCESSION NO.	3. RECIPIENT'S CATALOG NUMBER
4. TITLE (and Subtitle) Bearingless Helicopter Main Rotor Development Volume II - Combined Load Fatigue Evaluation of Weathered Graphite/Epoxy Composite		5. TYPE OF REPORT & PERIOD COVERED Final Report May 1975 CR- 145144 Dec. 1976
7. AUTHOR(s) Joseph J. Rackiewicz		6. PERFORMING ORG. REPORT NUMBER SER-72038
9. PERFORMING ORGANIZATION NAME AND ADDRESS Sikorsky Aircraft Division United Technologies Corporation Stratford, Conn. 06602		8. CONTRACT OR GRANT NUMBER(s) NAS1-13882
11. CONTROLLING OFFICE NAME AND ADDRESS National Aeronautics and Space Administration Washington, D.C. 20546		10. PROGRAM ELEMENT, PROJECT, TASK AREA & WORK UNIT NUMBERS
14. MONITORING AGENCY NAME & ADDRESS (if different from Controlling Office)		12. REPORT DATE
		13. NUMBER OF PAGES
		15. SECURITY CLASS. (of this report)
		15a. DECLASSIFICATION/DOWNGRADING SCHEDULE
16. DISTRIBUTION STATEMENT (of this Report)		
17. DISTRIBUTION STATEMENT (of the abstract entered in Block 20, if different from Report)		
18. SUPPLEMENTARY NOTES		
19. KEY WORDS (Continue on reverse side if necessary and identify by block number)		
20. ABSTRACT (Continue on reverse side if necessary and identify by block number) Small scale combined load fatigue tests were conducted on six arti- ficially and six naturally weathered test specimens. The test specimen material was unidirectionally oriented A-S graphite - woven glass scrim - epoxy resin laminate previously fabricated under NASA Contract No. NAS1- 12662 and reported in Reference (1).		

(over)

After weathering the laminate, specimens were prepared for testing. Two loading conditions with specific combinations of steady axial, vibratory torsion, and vibratory flatwise/edgewise bending as previously tested and reported in Reference (1) were selectively chosen. Test stress levels were varied up to a maximum of 3.5 times the baseline stress levels described in Reference (1). At the specific combined load flight stress levels and conditions tested, the percent of fatigue damage to both artificially and naturally weathered test specimens tested herein was similar to the damage experienced by non-weathered test specimens; and, under the conditions evaluated, the effect of weathering was negligible. The damping and natural frequency measurements on weathered specimens showed that a consistent and realistic increase in damping and a reduction in natural frequency after 10^7 fatigue cycles occurred only in specimens where interlaminar matrix cracking was detected by ultrasonic 'C' scan. Significant and meaningful identical proportional changes were detected when comparing both torsional damping and natural frequency changes to the torsional modulus changes even at percentages less than 5%. While the NDI technique utilizing ultrasonic 'C' scan did provide an excellent means for detecting longitudinal interlaminar cracking defects, the dye penetrant technique was a more useful inspection method for detecting minor surface cracks.

FORWARD

This document was prepared by Sikorsky Aircraft Division of United Technologies Corporation under Contract NAS1-13882 to the National Aeronautics and Space Administration and USAAMRDL of the Langley Directorate. It is subdivided into two volumes as follows:

Volume I Design and Test Evaluation of Large Scale Composite Bearingless Main Rotor Flexbeam

Volume II Combined Load Fatigue Evaluation of Weathered Graphite/Epoxy Composite

This report covers work conducted during the period of May 1975 to December 1976.

TABLE OF CONTENTS

<u>SECTION</u>	<u>PAGE</u>
SUMMARY	1
INTRODUCTION	2
LIST OF TABLES	3
LIST OF FIGURES	4
MATERIALS, EQUIPMENT AND PROCEDURES	6
Materials and Test Specimen Configuration	7
Equipment and Procedures	7
Torsional and Flexural Modulus Calibrations	7
Damping and Frequency Calibrations	8
Non-Destructive Inspection Techniques	8
Ultrasonic 'C' Scan	8
X-Ray Radiography	9
Dye Penetrant	9
Combined Load Fatigue Tests	9
Test Conditions	10
Weathering Tests	10
RESULTS AND DISCUSSION	12
Combined Load Fatigue Tests	12
Damping and Natural Frequency Measurements	14
Failure Analysis	14
X-Ray Radiography	14
Dye Penetrant	14
Ultrasonic 'C' Scan	15
Natural and Artificial Weathering	16
CONCLUSIONS	17
RECOMMENDATIONS FOR FURTHER STUDIES	18
REFERENCES	19

SUMMARY

Small scale combined load fatigue tests were conducted on six artificially and six naturally weathered test specimens. The test specimen material was unidirectionally oriented A-S graphite - woven glass scrim-epoxy resin laminate previously fabricated under NASA Contract No. NAS1-12662 and reported in Reference (1).

After the laminate was weathered, specimens were prepared for testing. Two loading conditions with specific combinations of steady axial, vibratory torsion, and vibratory flatwise/edgewise bending as previously tested and reported in Reference (1) were selectively chosen. Test stress levels were varied up to a maximum of 3.5 times the baseline stress levels described in Reference (1). At the specific combined load flight stress levels and conditions tested, the effect of weathering was negligible. Further, the percent of fatigue damage to both artificially and naturally weathered test specimens tested herein was similar to the damage experienced by non-weathered test specimens. The damping and natural frequency measurements on weathered specimens showed that a consistent and realistic increase in damping and a reduction in natural frequency after 10^7 fatigue cycles occurred only in specimens where interlaminar matrix cracking was detected by ultrasonic 'C' scan. Significant and meaningful identical proportional changes were detected when comparing both torsional damping and natural frequency changes to the torsional modulus changes even at percentages less than 5%. While the NDI technique utilizing ultrasonic 'C' scan did provide an excellent means for detecting longitudinal interlaminar cracking defects, the dye penetrant served as a useful inspection method for detecting surface cracks.

INTRODUCTION

The purpose of this effort was to assess the effect of weathering on composite materials which are subjected to combined cyclic loads. To make this assessment combined load fatigue tests of artificially and naturally weathered small scale test specimens were conducted and compared to fatigue results of non-weathered specimens at some of the selected stress levels and conditions previously reported in Reference (1). These selected stress levels and conditions are outlined in Table I. All weathered specimen fatigue data was acquired by performing torsional and bending stiffness measurements at 0, 5×10^6 and 10^7 cycles.

In addition to performing visual damage inspection, an attempt was made to correlate damage detected by NDI methods of soft x-ray radiography, dye penetrant, and ultrasonic 'C' scan with damage viewed in photomicrographs of the test specimens at 0 and 10^7 fatigue cycles on the weathered specimens only. An attempt was also made to compare torsional damping and natural frequency measurement changes versus torsional stiffness change after 10^7 fatigue cycles on weathered specimens.

LIST OF TABLES

TABLE I	Artificially and Naturally Small Specimen Test Program . .
TABLE II	Requirements of SS-9611 and Certified Test Results for Type A/S Graphite Composite Materials
TABLE III	Modulus Reduction Data Comparing Artificial and Na- tural Weathered vs. Non-Weathered Specimens
TABLE IV	Damping and Natural Frequency Measurements as a Function of Fatigue Cycles
TABLE V	Comparison of Torsional Critical Damping (C/Cc) and Frequency (f) change Versus Torsional 'G' change after Fatigue Testing to 10 ⁷ Cycles
TABLE VI	Test Results Comparing Percent of Damaged Area Detected by Ultrasonic 'C' Scan Versus Torsional Modulus Reduction after 10 ⁷ Fatigue Cycles

LIST OF FIGURES

- FIGURE 1. Combined Load Test Specimen Configuration
- FIGURE 2. Fatigue Specimen Showing Strain Gage Locations
- FIGURE 3. Static Torsional Modulus Measurement Fixture
- FIGURE 4. Static Flexural Modulus Measurement Fixture
- FIGURE 5. Torsional Damping and Natural Frequency Measurement Fixture. . . .
- FIGURE 6. The Ultrasonic C-Scan Facility Equipped with an Automated Recording Device, Synchronized with the Transducer Motion
- FIGURE 7. Ultrasonic Calibration of Test Specimen was Accomplished with Machined Defect
- FIGURE 8. Combined Load Fatigue Test Facility
- FIGURE 9. Specimens Subjected to Weathering on Roof of the Sikorsky Aircraft Plant
- FIGURE 10. Accelerated Weathering Tests Conducted in Weatherometer
- FIGURE 11a. Weathered vs. non-weathered torsion test results for Condition 1
- FIGURE 11b. Weathered vs. non-weathered Torsion Test Results for Condition 2
- FIGURE 12a. Weathered vs. non-weathered Flatwise Bending Test Results for Condition 1
- FIGURE 12b. Weathered vs. non-weathered Flatwise Bending Test Results for Condition 2
- FIGURE 13. Test Results Showing the Comparative Changes in Torsional Modulus (G),⁷Critical Damping (C/Cc) and Natural Frequency (f) after 10⁷ Fatigue Cycles
- FIGURE 14. Detection of Fatigue Damage Cracking by Dye Penetrant Inspection
- FIGURE 15. Calibrated Specimen Showing the Four Scanning Directions taken at a 20° Angle Beam to the Specimen

LIST OF FIGURES (Cont.)

- FIGURE 16. Ultrasonic Straight Pulse Echo 'C' Scan Showing Percent Disbond area for each Fatigue Damaged Specimen
- FIGURE 17. Ultrasonic loss of Back Face 'C' Scan showing Percent Disbond area for each Fatigue Damaged Specimen
- FIGURE 18. Typical Artificial and Natural Weathering Effects showing Surface Resin Leach out-exposing Scrim Fibers

MATERIALS, EQUIPMENT AND PROCEDURES

Materials and Test Specimen Configuration

The material used for the weathered test specimens for this program was Hercules, Inc. type A-S graphite fiber with style 10⁴ woven glass scrim prepregged by Dexter Materials Corp. (now Reliable Mfg. Corp.) with DM-101 resin system. This modified epoxy resin system requires a cure temperature of 275°F (135°C) with the potential design operational temperature capabilities to 200°F (92°C). Certification tests were performed by the vendor in accordance with requirements of Sikorsky specifications standard SS-9611, Reference (2). The results of the certification tests and the requirements of Reference (2) are given in Table II. In general, this material met the requirements of Reference (2).

The fabrication of the test specimen laminate (without doublers) which were used for the weathering test conducted herein was completed in approximately the same time period as the non-weathered test specimen laminate as outlined in the test program of Reference (1). A 10 ply flat panel laminate approximately 12 in. (30.5 cm.) x 24 inches (61.0 cm.) was laid up then vacuum bagged and autoclave cured at 100 psi (6.9×10^5 N/m²) for 2 hours at 275°F (135°C). A nominal cured per ply thickness of .0095" (.024 cm.) was obtained, .0085 inches (0.022/cm.) A-S graphite and 0.001 inches (0.002cm.) 10⁴ style woven glass scrim. Prior to weathering, a total of 12 test specimens were rough cut from the laminate above at a width of 1 1/16 inch (2.70 cm.). During the course of 2 years the specimens were weathered and periodically weighed as described in section 2.2.6 of this report. After weathering was completed, specimens were cleaned with methyl ethyl ketone and loose surface scrim on the specimens was removed to provide a good bonding surface. Unidirectional (E-glass) fiberglass doublers were individually bonded to the graphite specimens using Hysol 9309.2 adhesive. The fiber orientation of both the graphite specimen and the fiberglass doublers was parallel to the long dimension (9.0 inches 23 cm.) of the specimen. The entire specimen was then ground to the final dimensions shown in Figure 1. The steel cuffs inserted at each end of the specimen and then placed in an alignment fixture which affixed the final test specimen length. The previously designed bolt hole pattern in the steel cuffs was then utilized as a drill jig in order to drill and locate the same bolt hole pattern in the graphite specimen. The specimen in the steel cuffs was then bolted together in the fatigue test specimen configuration shown in Figure 1.

Equipment and Procedures

Torsional and Flexural Modulus Calibrations

Strain gauges (350 ohm type) were bonded on all specimens in order to measure flatwise bending, edgewise bending and torsional properties, i.e. (load, stress, strain and modulus). A typical combined load specimen with end grip attachments and strain gages in place is shown in Figure 2. Both flatwise and edgewise bending gauges were located at the end of the nontapered fiberglass doubler where it had been previously determined that the maximum bending loads occur. In all cases the ratio of flatwise to edgewise stress was nearly constant along the entire length of the specimen. The torsional gauges were located in the middle of the specimen width and at a 3" distance from the end of the non-tapered doubler where the maximum torsional stress would occur.

The test fixture shown in Figure 3 was used to determine the torsional modulus and stiffness changes. The torsional modulus of each specimen was calculated by applying known torques to the specimen and the measuring the output strains from these torques. With each applied torque, the angle of twist was also recorded. The measurement of the changes in the angle of twist as a function of fatigue cycles provided the means of determining the percentage change in torsional modulus.

The test fixture shown in Figure 4 was utilized to determine both the flatwise and edgewise flexural bending modulus changes. The specimen was loaded as a cantilever beam and the outputs of the pure flatwise and pure edgewise bending strain gages were individually recorded. Each bending modulus was separately used rather than averages of the two in the combined load test set-up. The deflection for a known applied load was recorded similar to those recorded with torsional measurements. The measurement of the changes in deflection as a function of fatigue cycles was used to determine the percentage change in both flatwise and edgewise flexural bending stiffness which is expressed in terms of an effective modulus change.

Both torsional and bending specimen strain gauge outputs were monitored using a strain gauge bridge, amplifier and oscilloscope console. Prior to test initiation and during periodic specimen removal, the static and dynamic eccentric setting were recorded and repeated whenever the specimen was reinstalled. Both static and dynamic stresses were adjusted until they were within 3 percent of desired values.

Damping and Frequency Calibrations

Damping and natural frequency measurements were made on the apparatus shown in Figure 5. The specimen was installed with one fixed end (top) while the other end was attached to a radial accelerometer. The specimen was then twisted so that the peak shear stress did not exceed 2000 psi. When released it produced an oscillation and amplitude which then was allowed to diminish in free decay. The output of the radial accelerometer was recorded using an oscillograph recorder.

In order to accurately measure the natural frequency of the specimen a reference signal was also recorded. The decay of the natural frequency as a function of cycles was utilized to calculate the ratio of damping capacity, C , to critical damping capacity C_c . The static measurements of the torsional modulus G as well as damping and frequency measurements were taken at 0 , 5×10^6 and 10^7 fatigue cycles.

Non-Destructive Inspection Techniques

Ultrasonic 'C' Scan

This work was accomplished at Pratt and Whitney Research Lab, East Hartford, Conn. The flat specimens were scanned automatically using the apparatus shown in Figure 6 which provided a 'C' scan printout. The 'C' scans are plan views of the flat specimens and are obtained by driving a writing device synchronously with the transducer. A mark is then made on the electrosensitive paper at any point where a signal is received on the ultrasonic instrument.

All ultrasonic work was conducted while the specimens were immersed in water. The amplitude of the signal at which the 'C'-scan would print defect indications was determined by using a calibrated flat specimen which had specific notches (created mechanically) as shown in Figure 7. The smallest notches designated in Figure 7 as areas 1, 2, 3 and 4 were approximately .28" (.71cm.) long, .035" (.089 cm.) wide and at depths of .013" (.033 cm.) for areas 1 and 2 and .020" (.051 cm.) for areas 3 and 4. The hole designated in Figure 7 as area 5 was approximately .045" (.114 cm.) deep and .125" (.318 cm.) in diameter. In all cases, the .013" (.033 cm.) notch was the smallest signal which could be readily differentiated from the background and set a lower limit on the size of the defect which can be detected. Ultrasonic 'C' scan were taken of both artificially and naturally weathered specimens before and after fatigue cycling.

X-Ray Radiography

The x-ray radiography was performed using 'soft' x-rays approximately 25 KVP (peak kilovolts) with a beryllium window in a normal laboratory air environment. Exposure time was approximately 3 minutes at 10 MAM (milliamperere minutes) using M type film. The source to film distance (SFD) was 18 inches (45.72 cm.) The x-rays were taken of each specimen (including calibration standard) before and after fatigue cycling. The x-rays were taken at several angles including normal to the specimen surface in order to cover all possible orientations of defects.

Dye Penetrant

Dye penetrant was used to detect surface damage after the specimen was fatigue tested to 10^7 cycles. The technique first involved cleaning the specimen with Spotcheck™ cleaner-type SKC-NF, second, coating the specimen with Spotcheck™ dye penetrant type SKL-HF and third, drying the specimen for 3 to 5 minutes. Excess penetrant was then removed with clean cheesecloth saturated with the same Spotcheck cleaner. Spotcheck™ developer type SKD-NF was then sprayed over specimen surface in the same area covered by dye penetrant. All surface defects were photographed subsequent evaluation of the defect size. All specimens were then thoroughly cleaned of all penetrant.

Combined Load Fatigue Tests

A combined load fatigue machine, was utilized to perform tests under varying combinations of steady axial, vibratory torsional and vibratory bending loads. Details of this machine are shown in Figure 8. As seen in Figure 8, the bending loads are applied by two bending eccentrics. The offset of each eccentric can be varied to control not only the bending stress distribution along the entire specimen length but also the maximum amplitude of the bending stress.

The ratio of edgewise stress to flatwise bending stress is controlled by adjusting the angle of the plane of the specimen with respect to the bending plane on the machine. For example, if the application of pure flatwise bending load is desired, then the angle between plane of the specimen and the bending plane of the machine is set at 90 degrees. Increasing the amounts of edgewise by varying the 90° angle until bending becomes pure edgewise at an angle of 0 or 180 degrees. The torsional

Combined Load Fatigue Tests (Cont.)

stress on the specimen is controlled by the third eccentric as shown in Figure 8. All three eccentrics are linked together by means of synchronized timing belts so that the maximum torsional and bending stress occur simultaneously. It has been previously demonstrated that this motion simulates both the cyclic torsional and bending stress experienced by the actual rotor blades.

A steady axial load simulating centrifugal force is also transmitted to the specimen by means of disk springs.

Test Conditions

The original test conditions were based on the predictions of the stress distributions in a full scale bearingless composite main rotor blade. Reasons why initially three load conditions with four different percents of flight stress at each load condition were investigated are detailed in the Reference (1) report.

Based upon the results of the Reference (1) report and the limited quantity (12) of weathered test specimens available, only two test load conditions with three different percents of flight stress at each load condition were repeated. Table I outlines the test program.

Weathering Tests

The graphite specimens designated for the natural weathering environment were placed on the roof of the Sikorsky Aircraft plant located in Stratford, Connecticut for a two year period.

A fixture as shown in Figure 9 was fabricated in order to position the specimen at a 45° angle to the horizon, facing South. These specimens received continuous exposure (one side only) to the rain and sunlight of the typical Connecticut environment during the time period of September 1971 through September 1973.

The graphite specimens designated for the artificial weathering environment were placed in an Atlas Electric Devices Company Model XW Weatherometer shown in Figure 10.

Each specimen was rotated to expose the opposite face after each 300 hour exposure period since only one face of the specimens could be exposed at one time. Each specimen face received a total of 600 hours of exposure. A 600 hour exposure in the weatherometer was

Weathering Tests (Cont.)

equivalent to two years in a Florida environment. This typical Florida environmental conditions would consist of continuous 130°F (54°C) heat and ultraviolet radiation and water spray 20 minutes every 2 hours. All specimens were weighed at periodic intervals in order to monitor weight loss or gain due to weathering either natural or artificial.

Results and Discussions

Combined Load Fatigue Tests

The test stress levels for each load condition as well as the resulting changes in flexural and torsional moduli for both non-weathered and weathered test specimens are tabulated in Table III. A plot of retained torsional modulus as a function of vibratory torsional stress at 10^7 cycles for load conditions 1 and 2 is given in Figures 11a and 11b. Conversely; Figures 12a and 12b for load conditions 1 and 2 show a plot of retained torsional modulus as a function of vibratory flatwise bending stress at 10^7 cycles. It must be stated that while the data points plotted for both the artificially and naturally weathered specimens in Figures 11a through 12b represent the actual results of the individual tests for each load condition, the corresponding data points for the nonweathered specimens shown in Figures 11a through 12b which were originally reported in Reference (1) were changed slightly after re-evaluation of that data. In general, the re-evaluation was based upon the additional experience gained over the past 3 years and the current practices now in effect. Specifically, three changes were incorporated and are detailed and discussed next.

- 1) Re-examination of non-weathered specimens showed various degrees of apparent disbonding between the fiberglass doublers and the graphite specimen. This disbonding may have been the reason for not a single specimen exhibiting zero damage upon calibration even after the accumulation of 1×10^6 fatigue cycles in the investigation reported in Reference (1). The establishment of improved bonding techniques instituted since the time of the publication of Reference (1) report has been the corrective action taken.
- 2) In order to normalize all data, it was required to re-evaluate the torsional modulus values for the non-weathered specimens at the same linear strain and/or torsional load level as the weathered specimens.
- 3) Re-evaluation of the method for determining percent retention of torsional modulus was re-defined in order to conform with more realistic results that should be received. For example, it was discovered that with the previous method employed in Reference (1) report, the torsional modulus losses after 10^7 fatigue cycles could theoretically exceed 100% when in reality the physical evidence (photomicrographs, ultrasonic 'C' scan and torsional damping characteristics) did not show 100% damage or total disbond. With the incorporation of the

Combined Load Fatigue Tests (Cont.)

three procedural changes and techniques above, the comparison between non-weathered and weathered specimen results could then be affected.

Because the torsional modulus change was more significant than either the flatwise or edgewise modulus changes as a function of fatigue cycles, it was chosen as the dependent variable as shown in Figures 11a through 12b and will be discussed exclusively. As shown in Figures 11a and 12a for load condition 1, the test results show that both non-weathered and weathered specimens are not affected when tested at the 220 and 300% flight stress level. However, identical fatigue damage in terms of a 30% torsional stiffness loss is exhibited at 330% flight stress level. It therefore can be assumed that the point of zero damage level for all specimens tested for load condition 1 seems to occur slightly before the 300% flight stress level, as defined by Table III, is reached. Test results for load condition 2 as shown in Figures 11b and 12b show that the point of zero damage for all specimens occurs slightly after the 220% level of flight stress, as defined by Table III, is obtained.

At the 300% level of flight stress where a targeted torsional stress of 5,600 psi (38.7×10^6 N/m²) in Figure 11b is required, both naturally and artificially weathered test specimens exhibited the same amount of damage i.e. approximately 25%. The non-weathered specimens exhibited 6% damage at the 300% flight level stress. However, after re-evaluation of this data it was discovered that the stress level was actually 5,300 psi (36.5×10^6 N/m²) and is plotted at this point in Figure 11b.

At the 350% level of flight stress where a targeted torsional stress of 6,540 psi (45.1×10^6 N/m²) is required, re-evaluation of the non-weathered specimen results also showed that the 45% damage level reported was actually 6,200 psi (42.7×10^6 N/m²) which is also plotted in Figure 11b.

At 330% flight stress level, it would at first appear that the damage to the artificially weathered specimens is 15% greater than that exhibited by the naturally weathered specimens. However, a statement to the effect that artificially weathering may be more severe than natural weathering cannot be made because both types of weathered specimens provided results that were within the scatter band of the mean curve plotted for non-weathered specimens. Consequently both weathering environments appear to have had very little effect on the combined load properties as compared to non-weathered specimens.

Damping and Natural Frequency Measurements

The recorded damping and natural frequency measurements obtained for both naturally and artificially weathered specimens is tabulated in Table IV. Table IV also gives the values of the percentage change of f , the natural frequency and C/C_c , the ratio of damping capacity to critical damping capacity after 5×10^6 and 10^7 fatigue cycles. A comparison of the percent change of both ' f ' and ' C_c ' as a function of percent change in torsional modulus at 10^7 fatigue cycles is tabulated in Table V and plotted in Figure 13. Test results in Figure 13 show that the percent changes in ' G ', f , and C_c are the same for all vibratory stress levels for Condition 1.

The examination of the various vibratory stress levels for Condition 2 show that the percent changes in the ' G ', ' f ', and ' C_c ' values are also the same at the 3,510 psi (24.2×10^6 N/m²) vibratory stress level or at the 220% of flight stress level. Further examination of the remaining two vibratory stress levels show that there is a very close agreement between the total change in torsion modulus and C_c values while the percent change in natural frequency is about 15 to 20% higher than both the ' G ' and ' C_c ' values.

Failure Analysis

There were three non-destructive testing techniques employed in order to determine extent of damage to all specimens. These were the following; 'soft' x-ray radiography, dye penetrant, and ultrasonic 'C' scan. Destructive examination in the form of photomicrographs taken at NDI indications was used to verify the results of the three NDT techniques whenever possible.

A discussion on the relative merit or short-coming of each NDT method is next.

X-Ray Radiography

Even though several x-rays were taken with varying parameters of KVP, exposure time and MAM with the utilization of a calibration standard on damaged and undamaged specimens, overall results proved negative. Further work would be required in order to refine this technique so that it is applicable to the size of cracking damage incurred by the specimens.

Dye Penetrant

Dye penetrant inspection was performed on all test specimens in order to detect any minor non-visual cracking on any surface of the test specimen. Particular attention was given to small minor crack detection in two areas. These areas were the longitudinal or horizontal surface cracking between plies and the

Dye Penetrant (Cont.)

transverse or vertical cracking on the top and bottom surface of the specimen. It was anticipated that surface irregularities other than cracking, i.e. butted plies of graphite and/or scrim non-scrim areas would be screened out. These irregularities might lead to false indications of cracking.

The results of this test method show that surface irregularities were not detected. Minor longitudinal or horizontal surface cracking between plies was detected and provided an excellent clear sharp indication for subsequent photomicrographs as shown in Figure 14a. While ultrasonic 'C' scan could not detect transverse or vertical cracking on the top and bottom surface of the specimen as will be discussed in detail in Section 3.3.3, dye penetrant did prove successful. The examination of potential surface cracks in three specimens as shown in Figure 14b revealed (through photomicrographs) that these cracks did exist.

This NDT technique appears to be a viable tool for detecting minor surface cracking on A-S graphite/epoxy composites.

Ultrasonic 'C' Scan

Two separate ultrasonic techniques 'Straight Pulse Echo' (SPE) and "Loss of Back Face" (LOBF), were employed in order to detect defects in the flat specimens at as many orientations as possible. With the above techniques, there were a total of five scanning directions investigated.

Four of these scans were at a 20° angle with a transducer distance of 2.25" (5.72 cm.) to the specimen surface. Figure 15 illustrates the calibrated specimen with defects and each of the four directional 20° angle scans taken. These scans were taken with the intention of detecting vertical cracking defects in the tested specimens, however the results of these four scanning orientations proved to be inconclusive.

The fifth and remaining scan was directed normal to the specimen surface. The transducer to specimen surface distance was 1 1/2 inches. (3.81 cm.). A 15 MHz transducer was employed for the scan. This scan successfully detected the horizontal cracking defects (areas of disbond) in all fatigue damaged specimens. The results of this scan are contained in Figure 16 and 17, 'Straight Pulse Echo' and 'Loss of Back Face' respectively.

Ultrasonic 'C' Scan (Cont.)

To subjectively evaluate both of the above methods, each specimen's ultrasonic scan was read in terms of total disbond area versus solid laminate. This quantitative technique was accomplished by means of a PlainometerTM which measures surface area in any direction. The percent disbond versus solid laminate area measured by the Plainometer utilizing both 'SPE' and 'LOBF' is tabulated in Table VI. Also given in Table VI is the percent torsional modulus retention after 10⁷ fatigue cycles for each damaged specimen.

An attempt was made to correlate torsional stiffness loss with percent total disbond area utilizing either 'SPE' or 'LOBF'. Results of this evaluation showed that only specimen numbers -16, -17 and -23 were comparable utilizing the 'SPE' technique while no specimens were comparable utilizing the 'LOBF' technique. Since data from only 3 out of 7 specimens give comparable results, no definite relationship seems to exist as to the potential comparison between the torsional stiffness loss with percent disbond. Of the two methods employed, 'SPE' provided a clearer and more precise representation of fatigue damage to the specimens.

Natural and Artificial Weathering

One of the conclusions given in Reference (1) report stated that the percent moisture gain after 600 hours of artificial and 143 days of natural weathering was less than 1 percent by weight. However, it was also stated that less than one percent of the total specimen weight was lost as a result of resin leaching out. It is therefore safe to state that the effect of moisture gain with this laminate after the time exposure with the above weathering conditions as reported in Reference (1) may have been obscured because of the weight loss due to resin leaching out. Because of this phenomenon, as shown in Figure 18, the naturally weathered specimen after given an additional exposure of 587 days again exhibited less than 1 percent moisture weight gain. Since each naturally weathered specimen produced randomly scattered results, the exact measurement of the percent of moisture gain after 2 years of exposure for naturally weathered specimen could not be accurately determined due to weight loss exhibited by resin leaching out of the specimen during the course of 2 years.

Conclusions

- 1) For stress levels up to 3.5 times or 350% predicted flight stresses, combined load fatigue testing of both types of weathered specimens produced the same amount of fatigue damage as non-weathered specimens.
- 2) Test results on all specimens showed that fatigue damage as indicated by torsional stiffness loss (approx. 30%) was only evident at 3.5 times the level of flight stress of condition 1, while the first indication of fatigue damage at condition 2 was evident at 3.0 times level of flight stress (30%) with a subsequent increase to 45% at 3.5 times level of flight stress.
- 3) 'C' scan with the pulse directed normal to the specimen surface can successfully detect the total area of disbond created by interlaminar longitudinal or horizontal cracking. Correlation between torsional stiffness loss and percent disbond was not able to be achieved.
- 4) The dye penetrant successfully detected minor surface cracks which were later identified with photomicrographs as definite vertical cracks in the fatigue damaged specimens.
- 5) The change in the torsional stiffness loss (G) correlated with the change in critical damping ratio (C_c).
- 6) The percent of moisture gain by weight for naturally weathered specimen over a period of 2 years could not be accurately determined due to weight loss caused by resin leaching out of the specimens.

Recommendations for Further Studies

- 1) A larger quantity of both naturally and artificially weathered specimens at other weathering environments (different humidities and temperatures) should be fatigue tested in the combined load state in order to determine the effect of these other environments on the fatigue strengths of graphite-glass scrim epoxy composites.
- 2) Refinement of both NDT techniques, ultrasonic 'C' scan and soft x-ray radiographs, should be investigated as to the feasibility of detecting small microscopic vertical cracks.
- 3) The effect of moisture due to weathering on different resin systems prepregged on A-S graphite should be evaluated in terms of accelerated versus long term aging effects.

References

- 1) M.G. Ulitchny and J.J. Lucas, "Evaluation of Graphite Composite Materials for Bearingless Helicopter Rotor Applications, "Sikorsky Aircraft, NASA CR-132414, January 1974.
- 2) Sikorsky Standard SS-9611, Graphite Fiber/Resin Matrix Preimpregnated Material, dated September 3, 1974.

TABLE I

ARTIFICIALLY AND NATURALLY WEATHERED SMALL SPECIMEN TEST PROGRAM

Load Condition Description	Percent Of Flight Stress	Torsional Stress + PSI $\pm(N/m^2 \times 10^6)$	Flatwise Bending Stress + PSI $\pm(N/m^2 \times 10^6)$	Edgewise Bending Stress + PSI $\pm(N/m^2 \times 10^6)$	Axial Stress + PSI $\pm(N/m^2 \times 10^6)$	Stress Ratios		No. of Specimens Tested	
						Flatwise/ Edgewise	Flatwise/ Torsion	Artificially Weathered	Naturally Weathered
1 High Bending Moderate Torsion Low Axial	220	2,420 (16.7)	37,500 (258.4)	11,600 (79.9)	4,000 (27.5)	3.4/1	15.4/1	1	1
	300	3,300 (22.7)	51,500 (354.8)	15,100 (104.0)	4,000 (27.5)	3.4/1	15.4/1	1	1
	350	3,850 (26.6)	59,500 (409.9)	19,200 (132.3)	4,000 (27.5)	3.4/1	15.4/1	1	1
2 Low Bending High Torsion Moderate Axial	220	3,510 (24.2)	15,000 (103.4)	5,380 (37.1)	8,000 (55.1)	2.8/1	3.6/1	1	1
	300	5,610 (38.7)	20,400 (140.6)	8,080 (55.7)	8,000 (55.1)	2.8/1	3.6/1	1	1
	350	6,540 (44.9)	23,800 (164.0)	8,540 (58.8)	8,000 (55.1)	2.8/1	3.6/1	1	1

TABLE II

 REQUIREMENTS OF SS-9611 AND CERTIFIED TEST RESULTS
 FOR TYPE A/S GRAPHITE COMPOSITE MATERIALS

Property	SS-9611 Requirement	Certified Test Results from DMC*	
Resin Content	44 ± 3%	44.7%	
Volatile Content	1.0% Max.	0.2%	
Horizontal Shear At	PSI (Min.)** (n/m ² x10 ⁶)	PSI (Min.)** (n/m ² x10 ⁶)	
-67°F (55°C)	Room Temp. Value ±5%	13,800	95,137
70°F (21°C)	12,000 82.7	12,100	83,417
160°F (71°C)	>95% of Room Temp.Value	11,700	80,660
250°F (121°C)	>75% of Room Temp.Value	9,360	64,528
Longitudinal Flexural Strength At	PSI (Min.)** (n/m ² x10 ⁶)	PSI (Min.)** (n/m ² x10 ⁶)	
-67°F (55°C)	Room Temp. Value ±5%	198,200	1,366
70°F (21°C)	200,000 1,378	208,200	1,438
160°F (71°C)	>95% of Room Temp.Value	222,400	1,533
250°F (121°C)	>75% of Room Temp.Value	193,500	1,333
Longitudinal Flexural Modulus At	PSI ±6% (n/m ² x10 ⁹)	PSI (n/m ² x10 ⁹)	
-67°F (55°C)	Room Temp. Value ±5%	16.2x10 ⁶	111.7
70°F (21°C)	16.2x10 ⁶ 111.7	16.2x10 ⁶	111.7
160°F (71°C)	>95% of Room Temp.Value	17.3x10 ⁶	119.3
250°F (121°C)	>75% of Room Temp.Value	15.7x10 ⁶	108.2
Graphite Fiber Weight	Must Be Reported	19.46 gm/sq ft	209 gm/sq m.
Glass Fiber Weight	Must Be Reported	1.88	20.2

*Information Furnished by Dexter Materials Corporation

**Average of Five Test Specimens

TABLE III

MODULUS REDUCTION DATA COMPARING ARTIFICIAL AND NATURAL WEATHERED VS.

Load Condition	Percent of Flight Stress	Torsional Stress + PSI $\pm(N/m^2 \times 10^6)$	Flatwise Bending Stress + PSI $\pm(N/m^2 \times 10^6)$	Edge-wise Bending Stress + PSI $\pm(N/m^2 \times 10^6)$	Natural and Artificially Weathered								Non-Weathered						
					Specimen		Initial Modulus $\times 10^6$ PSI $(\times 10^9 N/m^2)$		Modulus Reduction at Cycles (Percent)				Specimen Number	Initial Modulus $\times 10^6$ PSI $(\times 10^9 N/m^2)$		Modulus Reduction at Cycles (Percent)			
							Tors.	Flex.	5×10^6		10^7			Tors.	Flex.	5×10^6		10^7	
					No.	Type	Tors.	Flex.	Tors.	Flex.	Tors.	Flex.	Tors.	Flex.	Tors.	Flex.	Tors.	Flex.	
1	220	2,420 (16.7)	37,500 (258.4)	11,600 (79.9)	-25	Art.	0.73 (5.0)	13.93 (96.0)	0.1	0.4	0.3	0.7	-04	0.73 (5.0)	14.20 (97.8)	0.0	2.0	0.0	5.7
					-16	Nat.	0.71 (4.9)	14.22 (98.0)	3.3	0.0	4.0	0.0							
1	300	3,300 (22.7)	51,500 (354.8)	15,100 (104.0)	-21	Art.	0.67 (4.6)	13.57 (93.5)	2.0	1.6	2.3	2.5	-06	0.71 (4.9)	13.33 (91.8)	0.0	2.5	0.0	5.0
					-18	Nat.	0.72 (5.0)	13.65 (94.0)	0.8	0.5	1.1	0.5							
1	350	3,350 (22.6)	59,500 (409.9)	19,200 (132.3)	-22	Art.	0.69 (4.8)	13.89 (95.7)	30.0	4.0	30.5	5.0	-08	0.69 (4.8)	13.30 (91.6)	9.9	0.0	35.8	6.5
					-19	Nat.	0.69 (4.8)	14.41 (99.3)	0.3	0.0	34.0	0.0							
2	220	3,510 (24.2)	15,000 (103.4)	5,380 (37.1)	-24	Art.	0.76 (5.2)	13.28 (91.5)	0.3	0.0	0.3	0.0	-09	0.69 (4.8)	13.70 (94.4)	0.0	0.5	0.0	2.5
					-15	Nat.	0.66 (4.5)	13.72 (94.5)	0.4	0.0	0.7	0.0							
2	300	5,610 (36.7)	20,400 (140.6)	8,080 (55.7)	-20	Art.	0.66 (4.5)	13.57 (93.5)	23.2	0.0	29.0	0.0	-05	0.70 (4.8)	13.36 (92.1)	5.6	1.9	5.9	2.9
					-17	Nat.	0.68 (4.7)	13.09 (90.2)	16.6	0.9	25.8	0.9							
2	350	6,540 (44.9)	23,800 (164.0)	8,540 (58.8)	-23	Art.	0.79 (5.4)	13.94 (96.0)	38.7	1.7	51.2	3.3	-07	0.69 (4.8)	14.06 (96.9)	33.5	1.5	45.0	3.9
					-14	Nat.	0.81 (5.6)	14.14 (97.4)	29.4	0.0	34.9	0.8							

NOTES: (1) For Load Condition 1 Axial Stress = 4000 PSI (27,596) N/m²
For Load Condition 2 Axial Stress = 8000 PSI (55,152) N/m²

(2) Data reprinted from NASA CR-132414, Table III

ORIGINAL PAGE IS OF POOR QUALITY

TABLE IV
DAMPING AND NATURAL FREQUENCY MEASUREMENTS AS A FUNCTION OF FATIGUE CYCLES

Specimen Number	Type of Weathered Specimen	Load Condition	Percent of Flight Stress	C/C _c and Frequency at Cycles						Percent Change of C/C _c and Frequency Compared to 0 Cycle Values, at Cycles			
				0		5 x 10 ⁶		10 ⁷		5 x 10 ⁶		10 ⁷	
				C/C _c X 10 ⁻²	Freq. Hz	C/C _c X 10 ⁻²	Freq. Hz	C/C _c X 10 ⁻²	Freq. Hz	C/C _c	Freq.	C/C _c	Freq.
-16	Natural	1	220	12.91	2.31	-	-	13.02	2.31	-	-	0.8	0.0
-21	Artificial	1	300	12.12	2.10	12.17	2.10	12.85	2.10	0.4	0.0	5.7	0.0
-19	Natural	1	350	13.02	2.31	-	-	16.66	1.70	-	-	21.8	26.4
-24	Artificial	2	220	12.70	2.01	-	-	13.10	2.01	-	-	3.1	0.0
-20	Artificial	2	300	11.72	2.09	-	-	19.49	1.58	-	-	39.9	24.4
-17	Natural	2	300	14.38	2.17	-	-	24.05	1.77	-	-	40.2	18.4
-23	Artificial	2	350	14.10	2.17	30.47	1.46	34.30	1.36	53.7	32.7	58.9	37.3
-14	Natural	2	350	12.72	2.07	-	-	21.64	1.36	-	-	41.2	34.3

TABLE V
 COMPARISON OF TORSIONAL CRITICAL DAMPING (C/C_c) AND FREQUENCY (f) CHANGE
 VERSUS TORSIONAL 'G' CHANGE AFTER FATIGUE TESTING TO 10⁷ CYCLES

SPEC. NO.	LOAD COND.	PERCENT FLIGHT STRESS	TORSIONAL STRESS ±PSI (±N/m ² x 10 ⁶)	FLATWISE BENDING STRESS ±PSI (±N/m ² x 10 ⁶)	EDGEWISE BENDING STRESS ±PSI (±N/m ² x 10 ⁶)	REDUCTIONS AT 10 ⁷ CYCLES		
						TORSIONAL MODULUS G (%)	FREQUENCY (%)	C/C _c (%)
-16	1	220	2,420 (16.7)	37,500 (258.4)	11,600 (79.9)	4.0	0.0	0.9
-21	1	300	3,300 (22.7)	51,500 (354.8)	15,100 (104.0)	2.3	0.0	5.7
-19	1	350	3,850 (26.6)	59,500 (409.9)	19,200 (132.3)	34.0	26.4	21.8
-24	2	220	3,510 (24.2)	15,000 (103.4)	5,380 (37.1)	0.3	0.0	3.1
-20	2	300	5,610 (38.7)	20,400 (140.6)	8,080 (55.7)	29.0	24.4	39.9
-17	2	300	5,610 (38.7)	20,400 (140.6)	8,080 (55.7)	25.8	18.4	40.2
-23	2	350	6,540 (44.9)	23,800 (164.0)	8,540 (58.8)	51.2	37.3	58.9
-14	2	350	6,540 (44.9)	23,800 (164.0)	8,540 (58.8)	34.9	34.3	41.2

ORIGINAL PAGE IS
 OF POOR QUALITY

TABLE VI

TEST RESULTS COMPARING PERCENT OF DAMAGED AREA DETECTED BY ULTRASONIC 'C'

SCAN VERSUS TORSIONAL MODULUS REDUCTION AFTER 10^7 FATIGUE CYCLES

Spec. No.	Total Area Inspected In ² (CM ²)	Straight Pulse Echo Inspection Results		Loss of Back Face Inspection Results		Percent Torsional Modulus Reduction (Ref. Table III)
		Total Disbond Area - In ² (CM ²)	Percent Disbond Area - %	Total Disbond Area - In ² (CM ²)	Percent Disbond Area - %	
-14	4.50 (29.03)	3.10 (20.00)	69.0	3.45 (22.26)	77.0	34.9
-16	4.93 (31.81)	0.23 (1.48)	5.0	1.45 (9.35)	29.0	4.0
-17	4.76 (30.71)	1.67 (10.77)	35.0	2.74 (17.68)	58.0	25.8
-19	4.67 (30.13)	3.00 (19.36)	64.0	3.07 (19.81)	66.0	34.0
-20	4.80 (30.97)	2.50 (16.13)	52.0	2.85 (18.39)	58.5	29.0
-22	4.82 (31.10)	3.60 (23.23)	75.0	2.85 (18.39)	59.0	30.5
-23	4.89 (31.55)	3.15 (20.32)	64.0	3.49 (22.52)	71.0	51.2

25

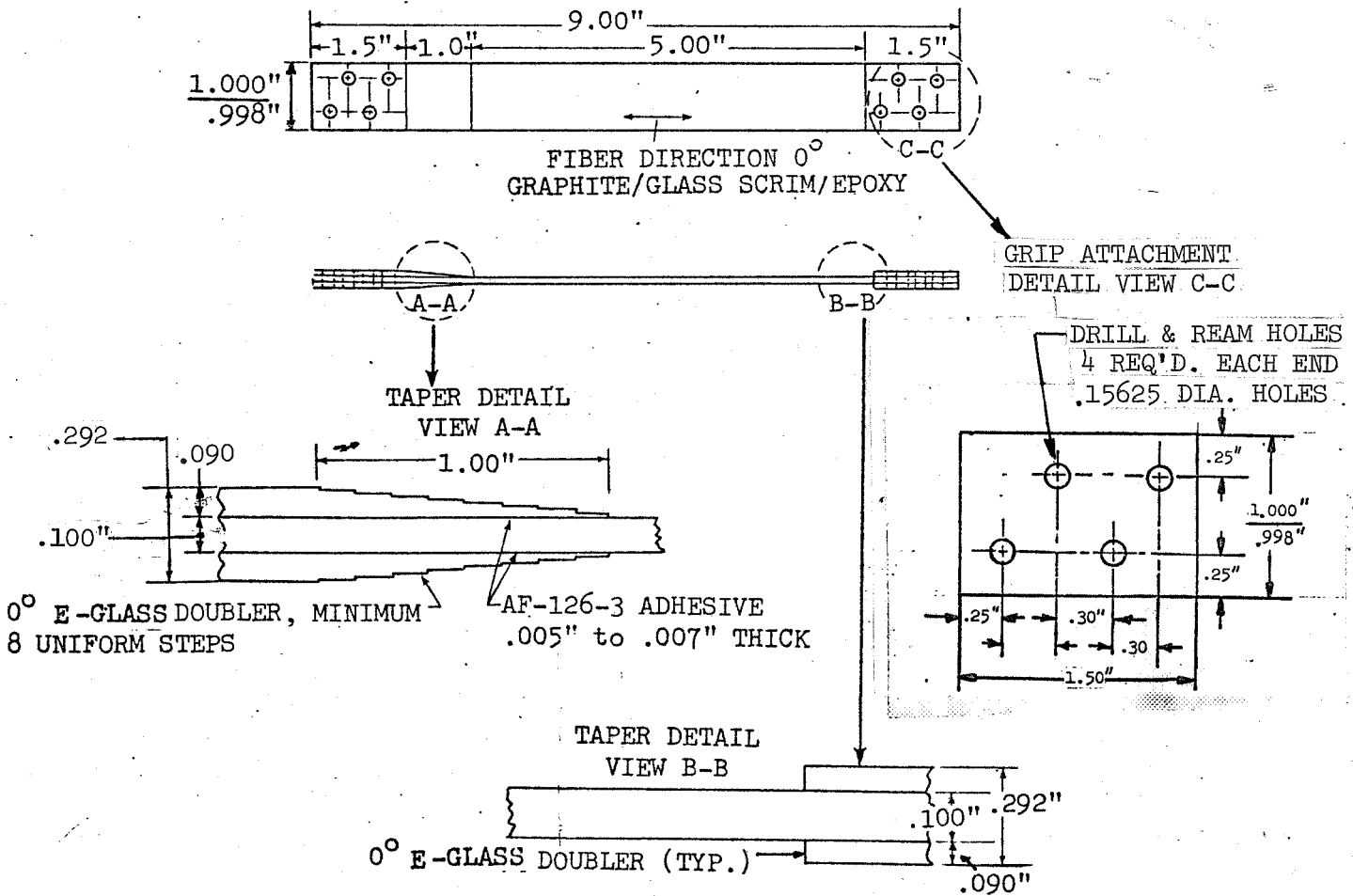
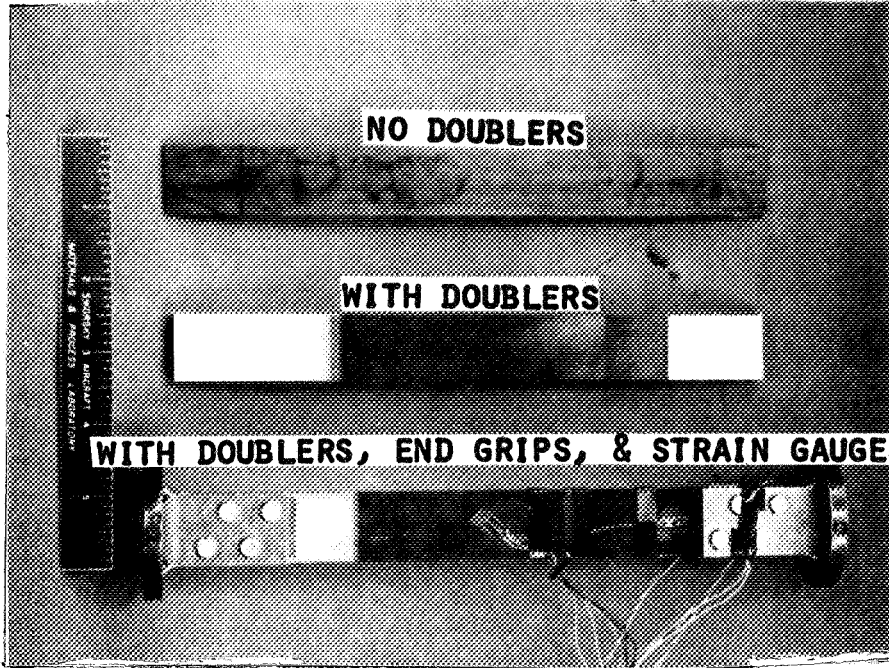


FIGURE 1
COMBINED LOAD TEST SPECIMEN CONFIGURATION

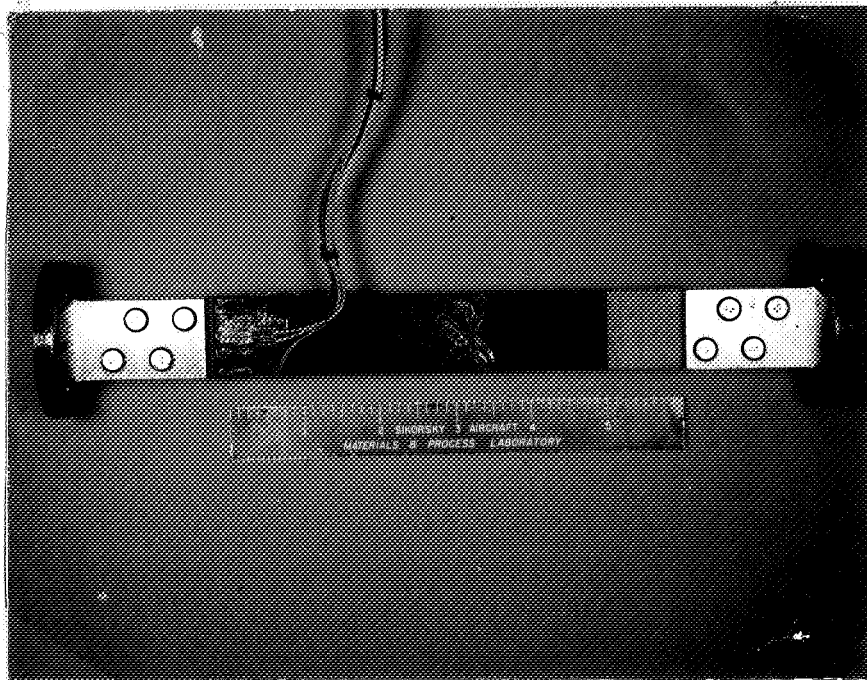
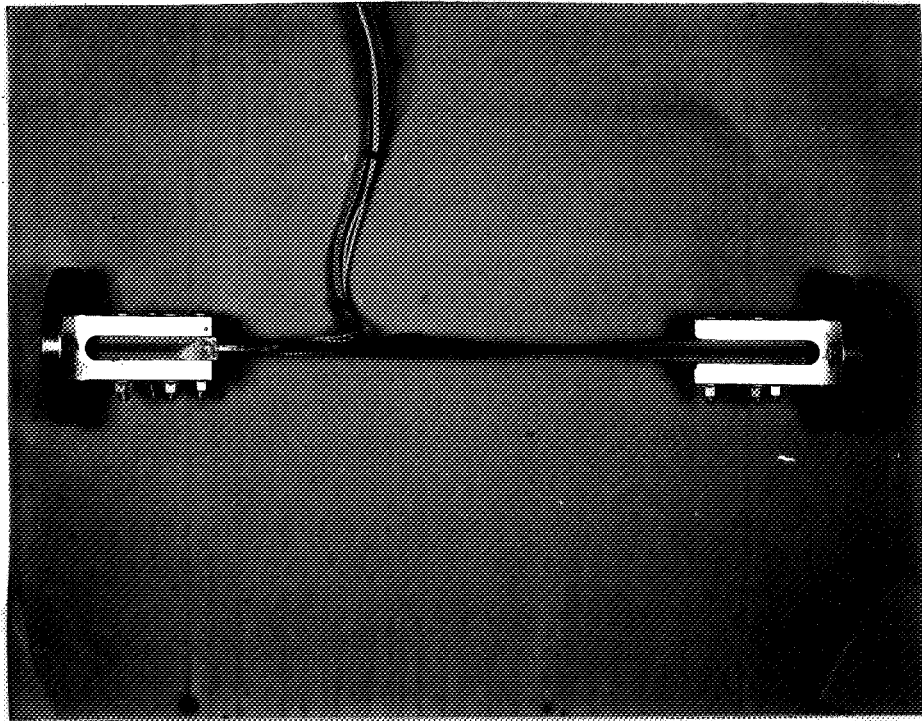


FIGURE 2
FATIGUE SPECIMEN SHOWING STRAIN GAGE LOCATIONS

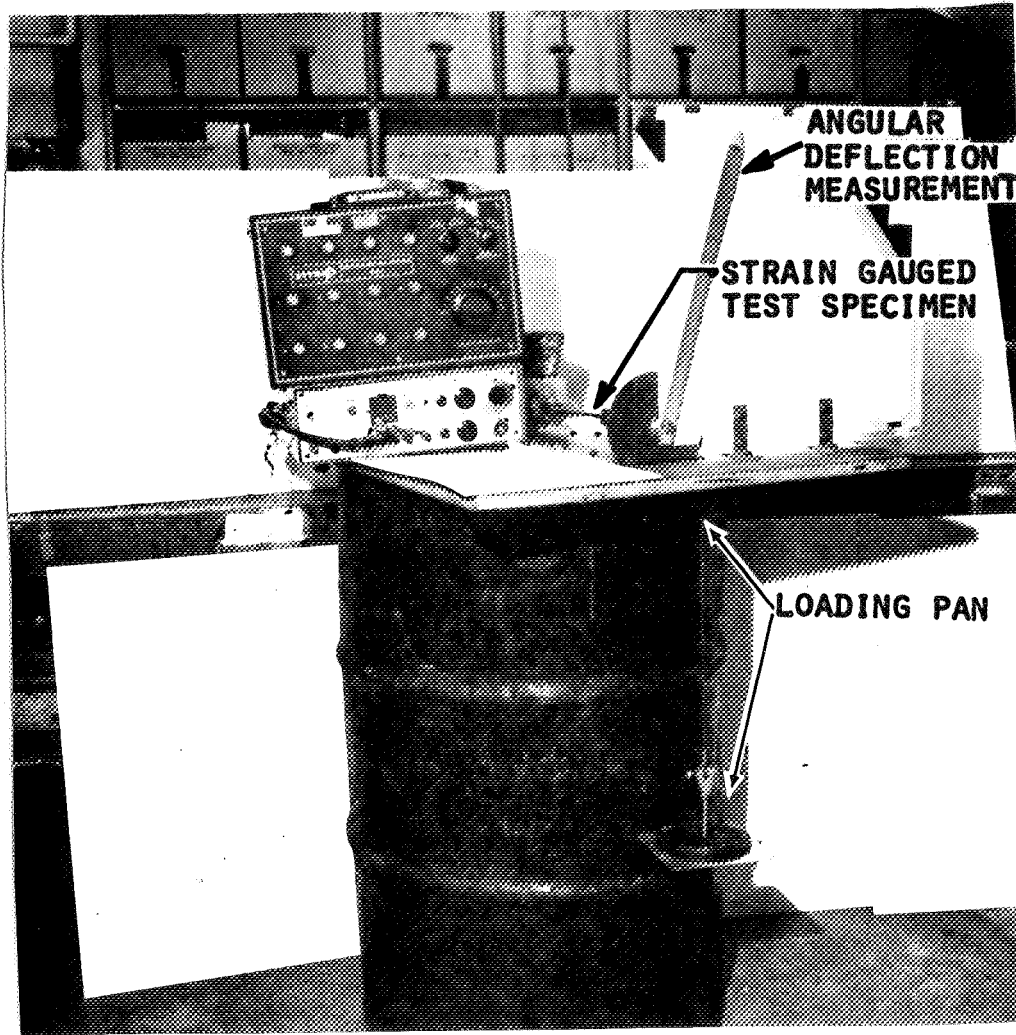


FIGURE 3
STATIC TORSIONAL MODULUS MEASUREMENT FIXTURE

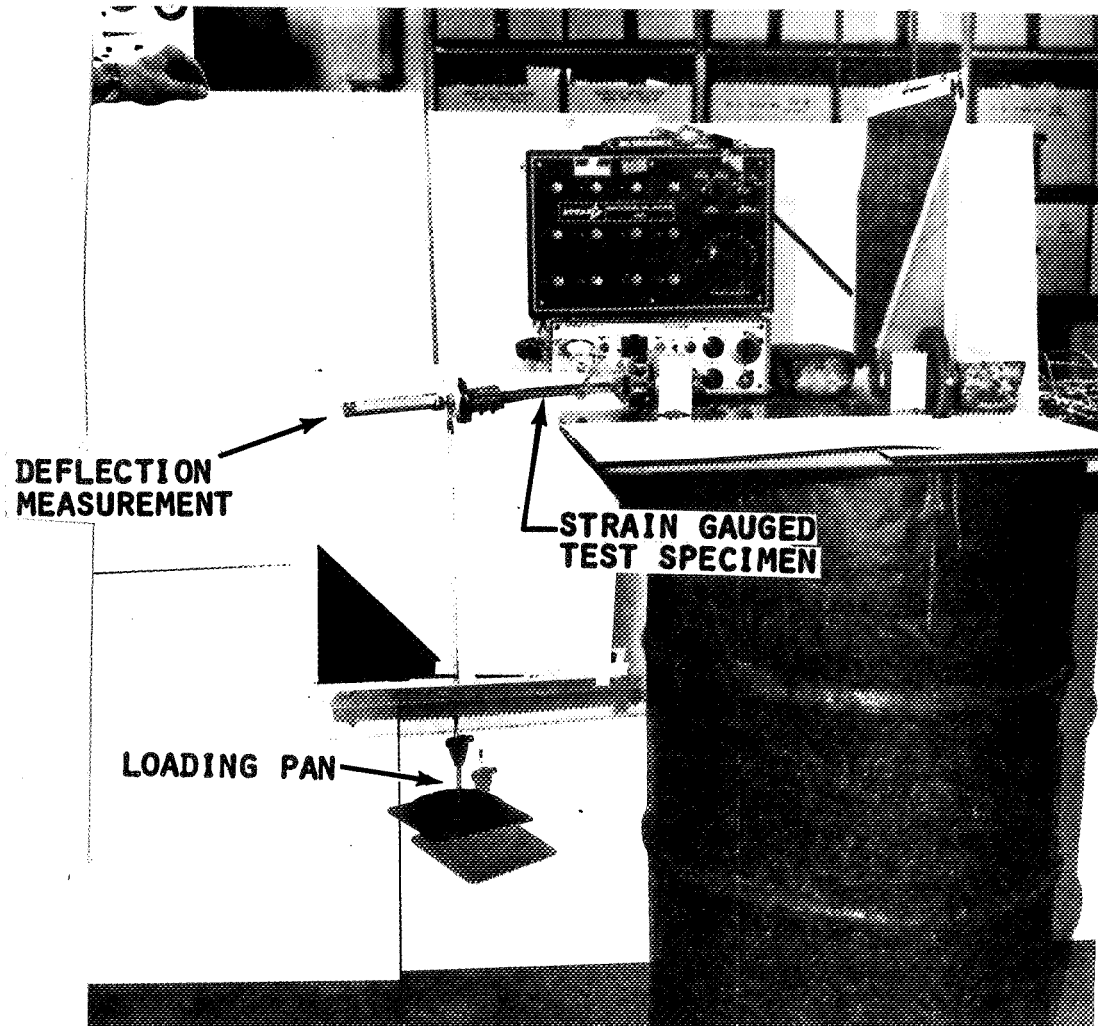
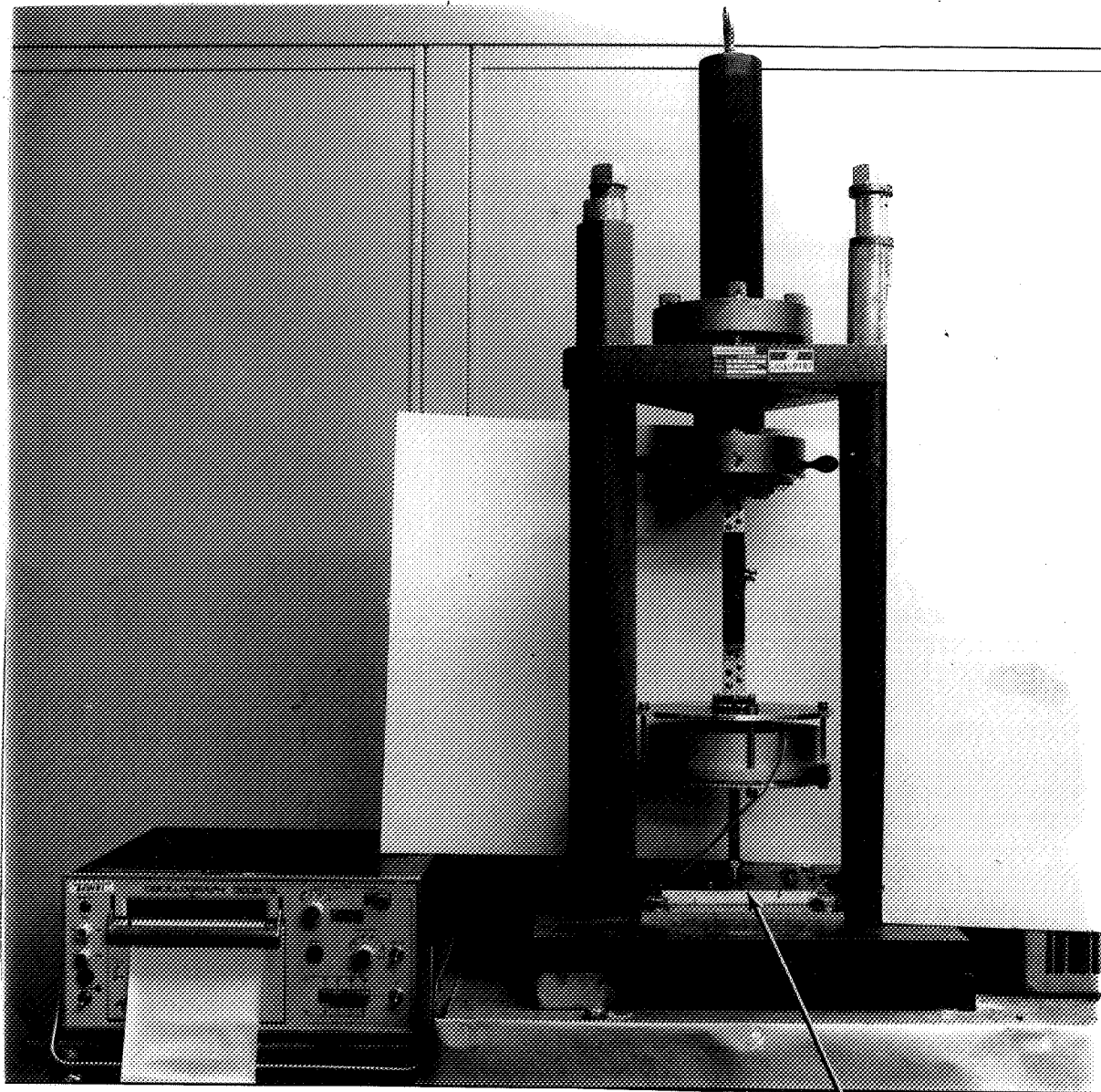


FIGURE 4

STATIC FLEXURAL MODULUS MEASUREMENT FIXTURE



RADIAL ACCELEROMETER

FIGURE 5

TORSIONAL DAMPING AND NATURAL FREQUENCY MEASUREMENT FIXTURE

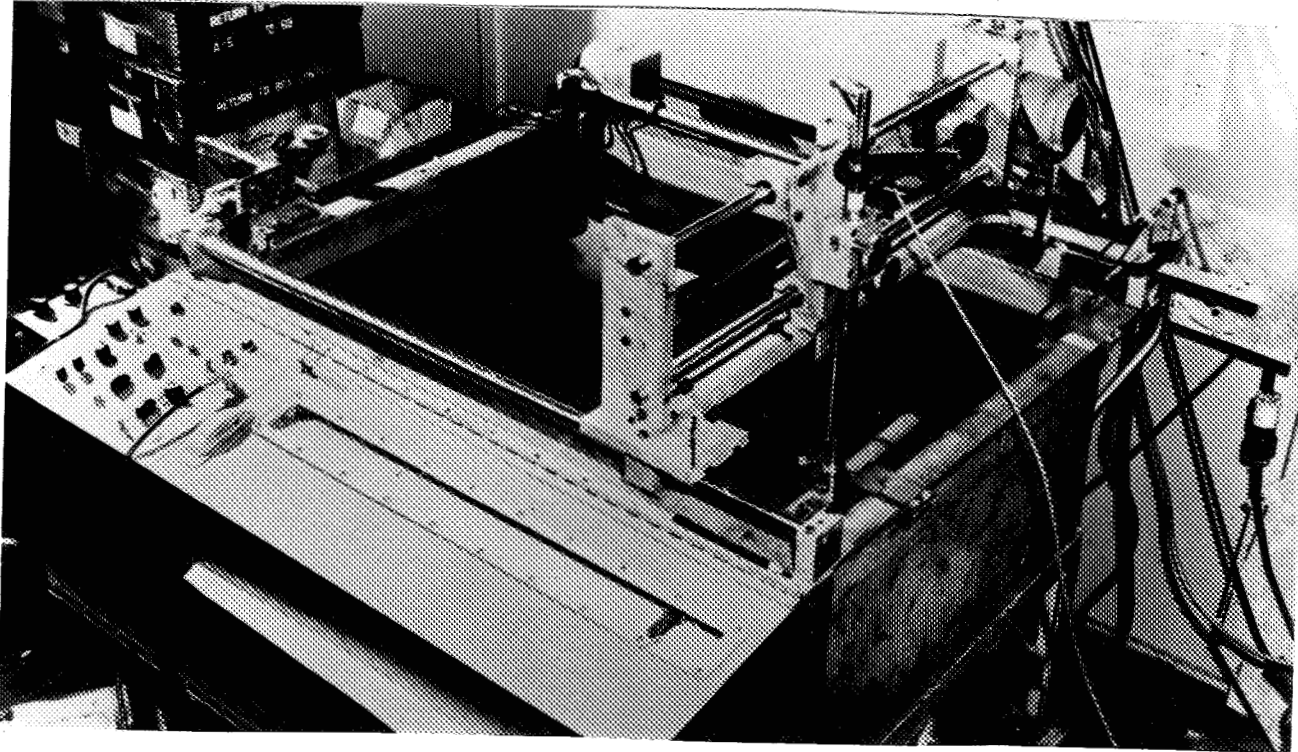
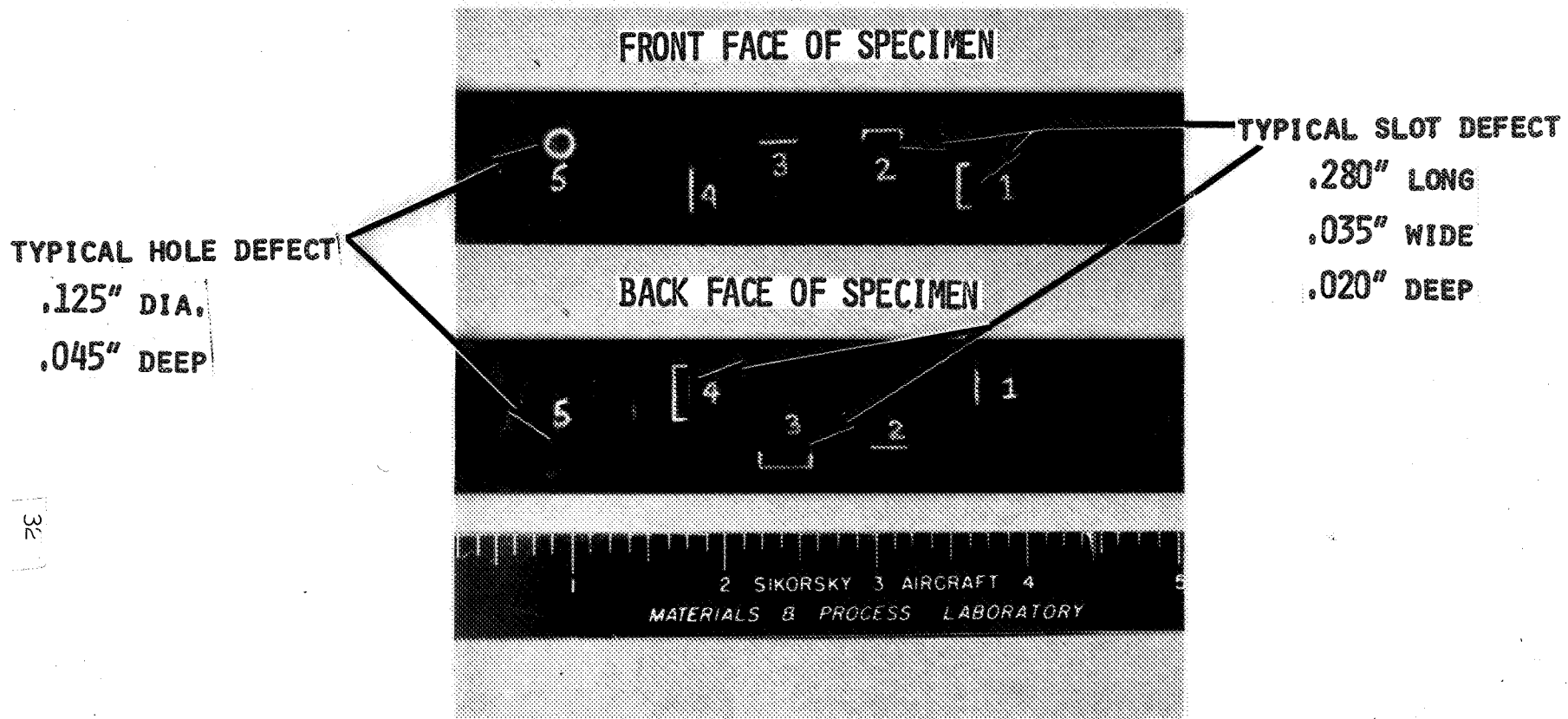


FIGURE 6

THE ULTRASONIC C-SCAN FACILITY EQUIPPED WITH AN AUTOMATIC RECORDING DEVICE, SYNCHRONIZED WITH THE TRANSDUCER MOTION



TYPICAL HOLE DEFECT
 .125" DIA.
 .045" DEEP

TYPICAL SLOT DEFECT
 .280" LONG
 .035" WIDE
 .020" DEEP

32

FIGURE 7

ULTRASONIC CALIBRATION OF TEST SPECIMEN WAS ACCOMPLISHED WITH MACHINED DEFECT

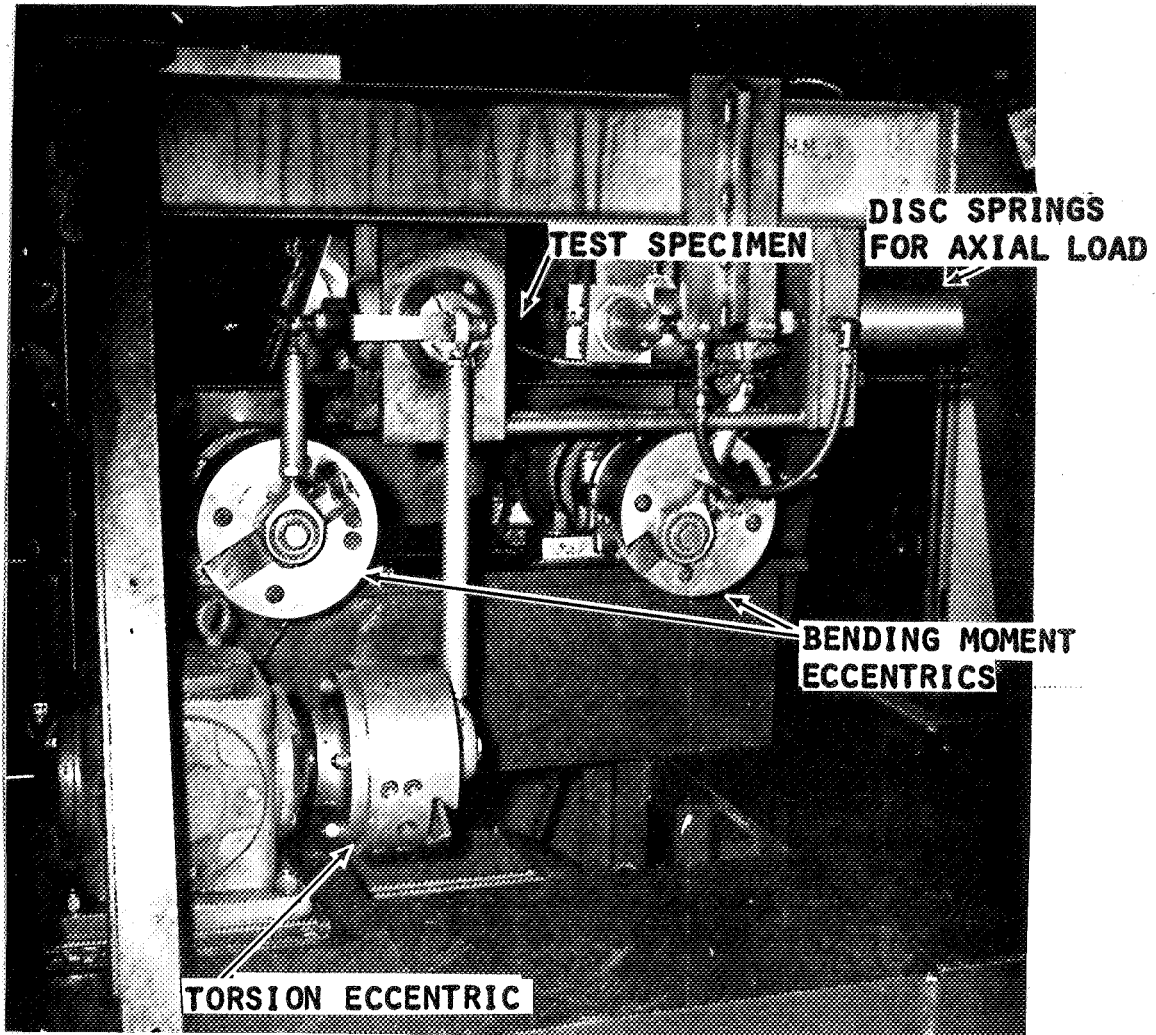


FIGURE 8

COMBINED LOAD FATIGUE TEST FACILITY

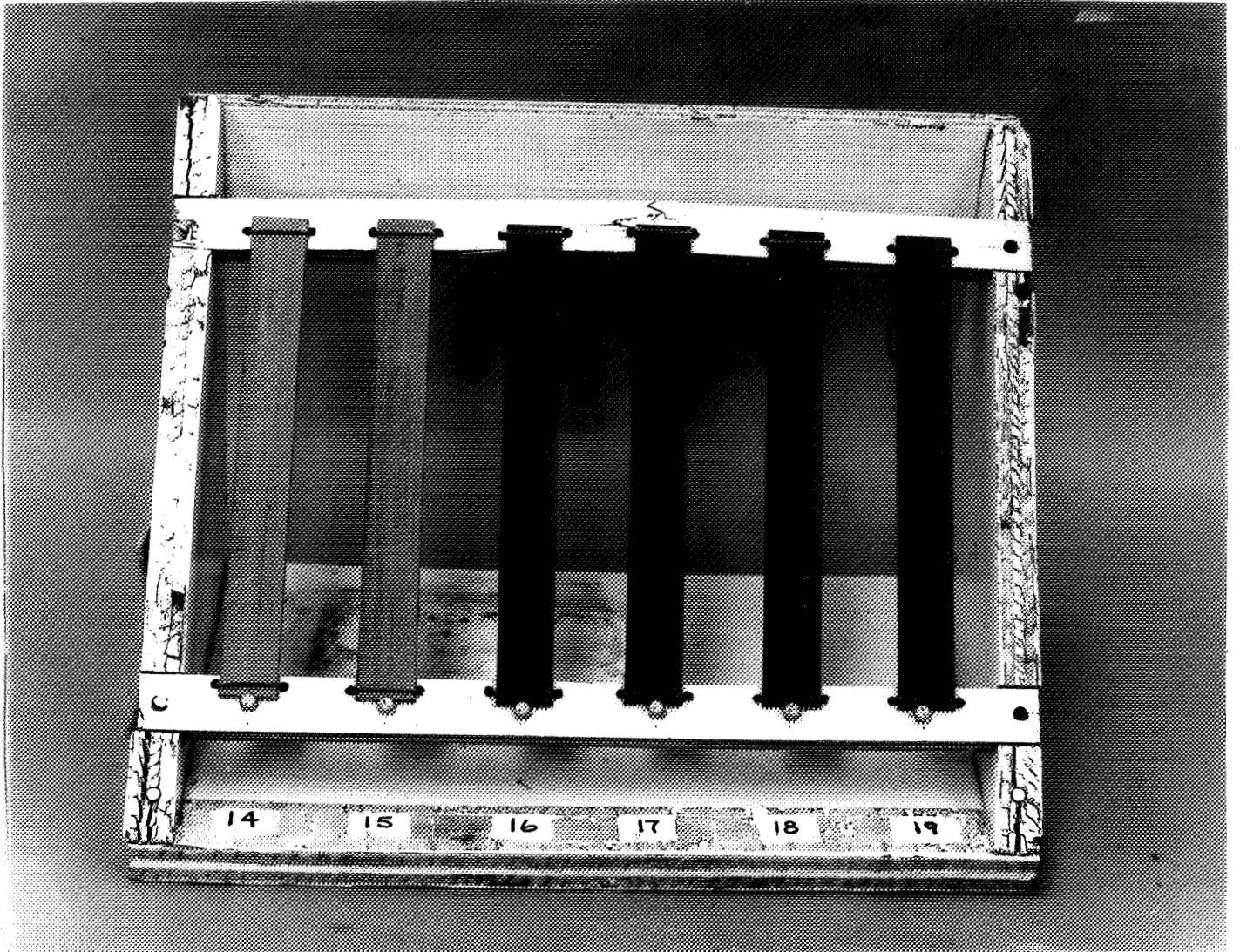


FIGURE 9

SPECIMEN SUBJECTED TO WEATHERING ON ROOF OF SIKORSKY AIRCRAFT PLANT

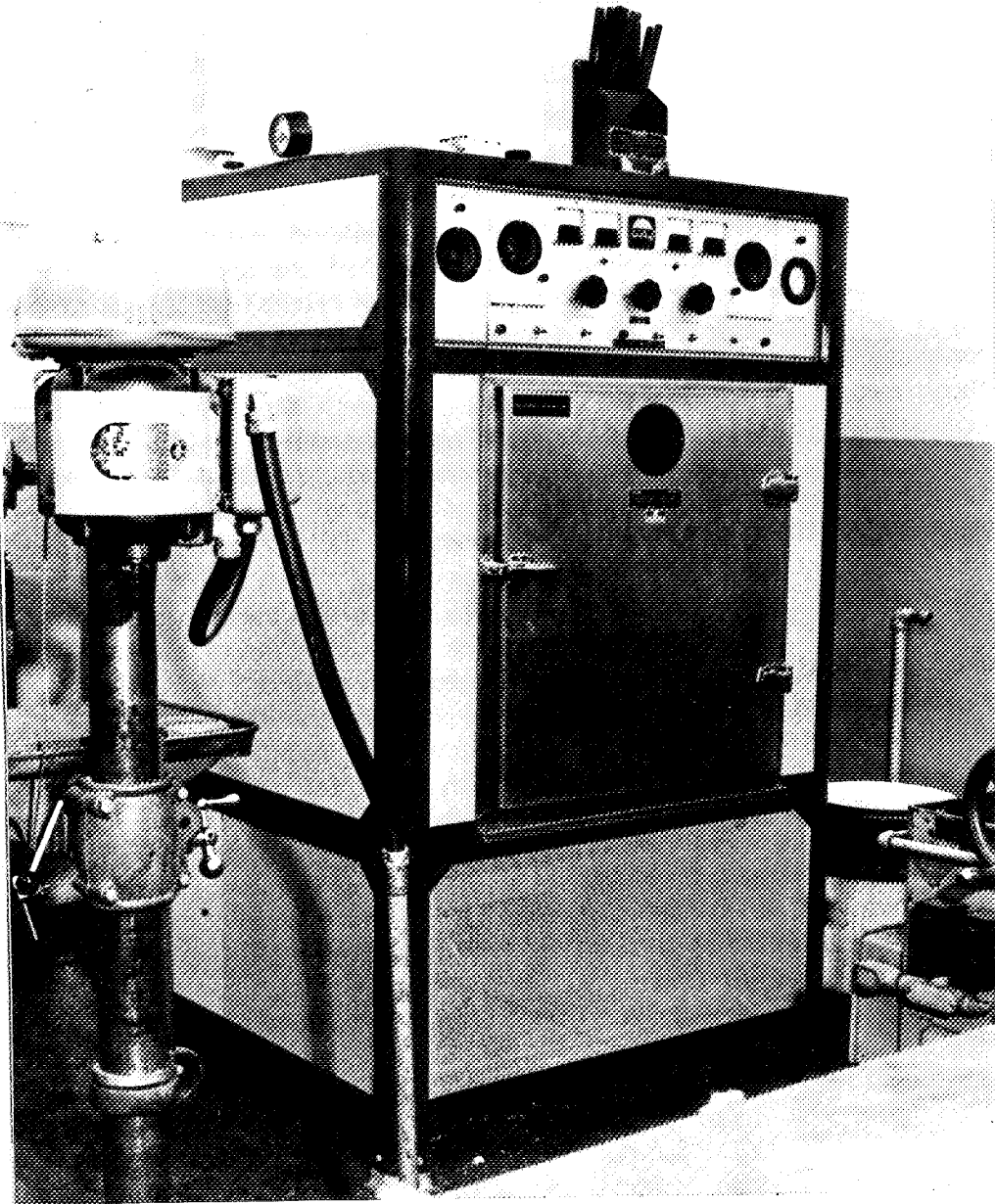


FIGURE 10

ACCELERATED WEATHERING TESTS CONDUCTED IN WEATHEROMETER

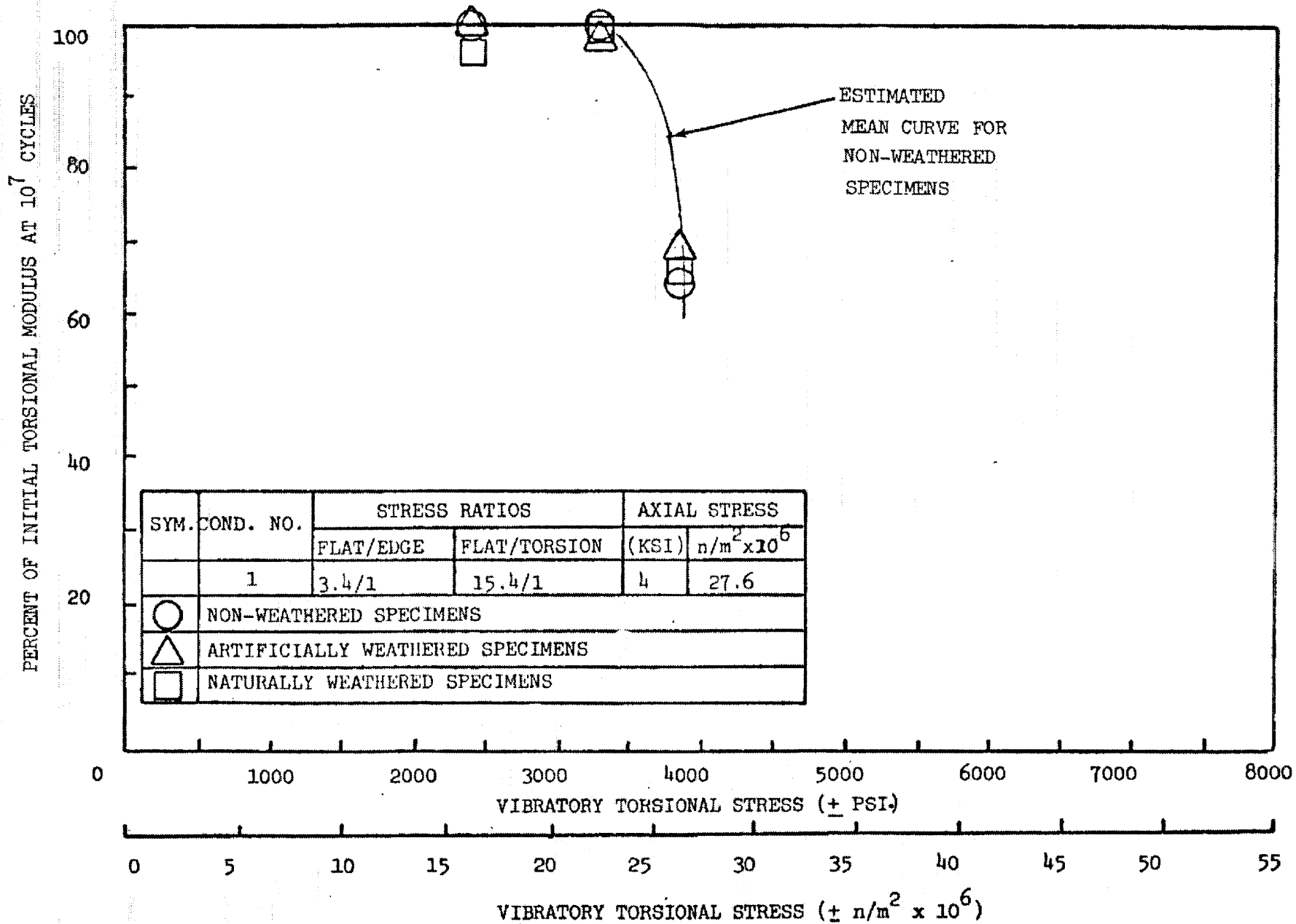


FIGURE 11a
 WEATHERED VS. NON-WEATHERED TORSION TEST RESULTS FOR CONDITION 1

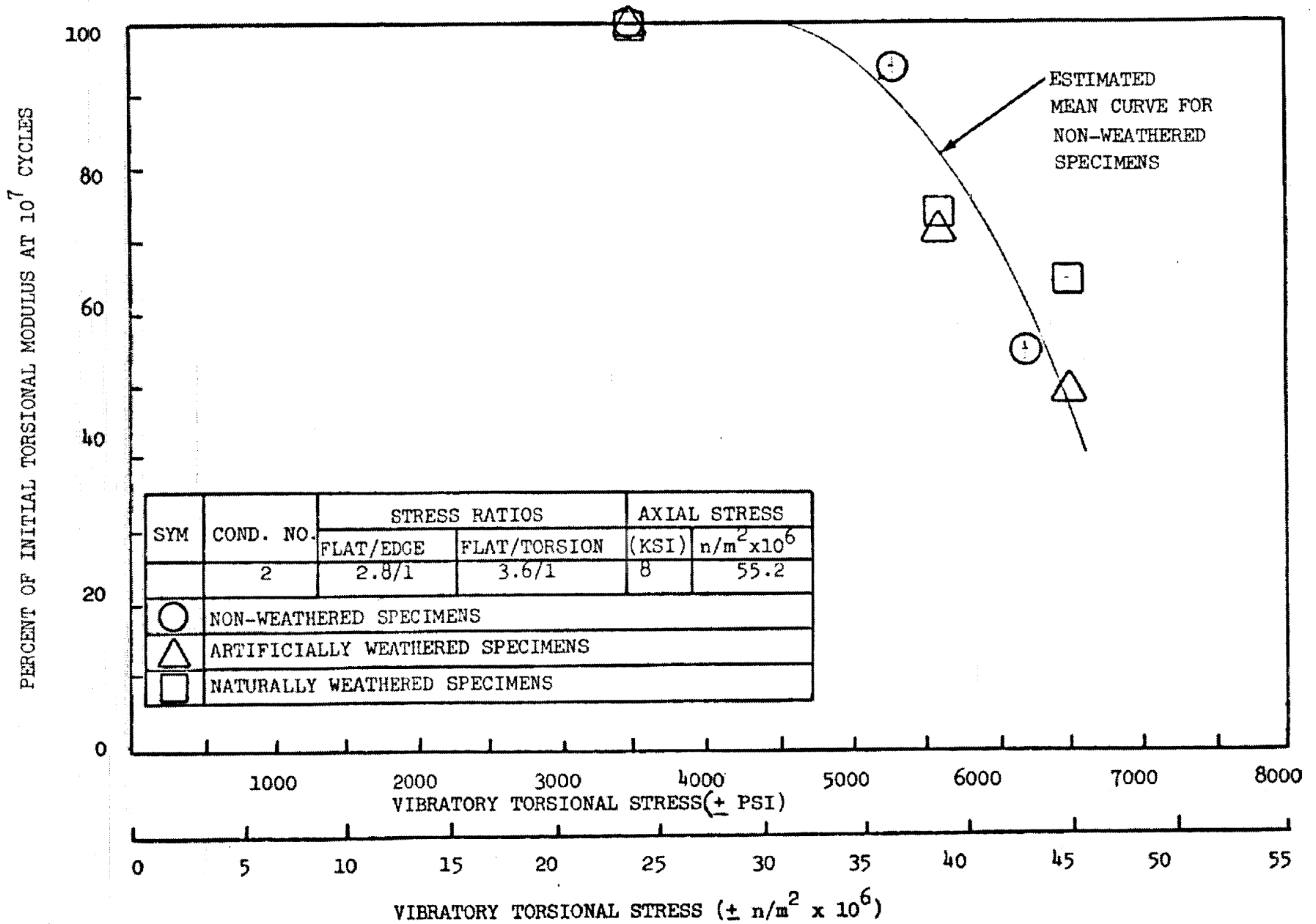


FIGURE 11b

WEATHERED VS. NON-WEATHERED TORSION TEST RESULTS FOR CONDITION 2

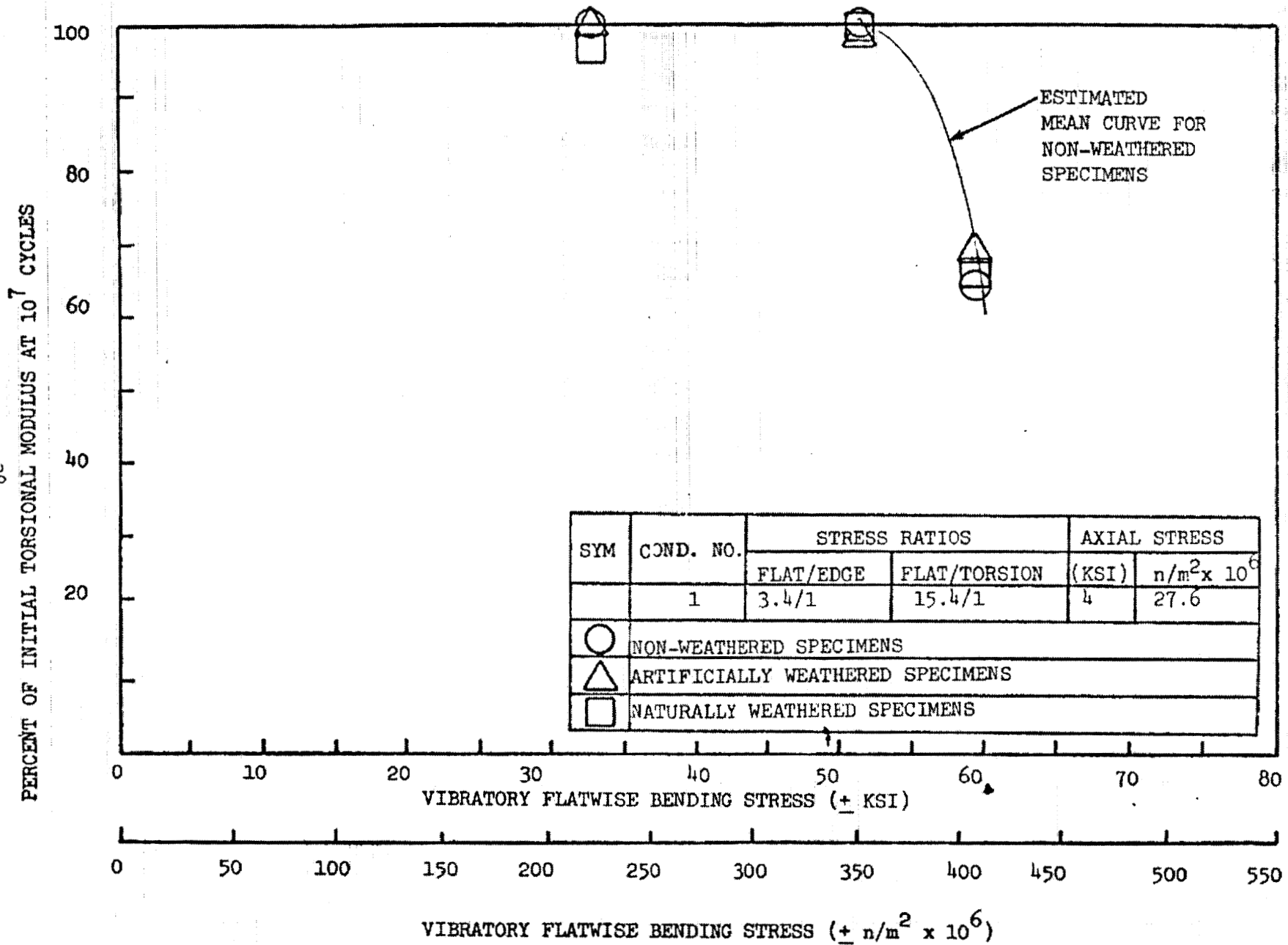


FIGURE 12a
 WEATHERED VS. NON-WEATHERED FLATWISE BENDING TEST RESULTS FOR CONDITION 1

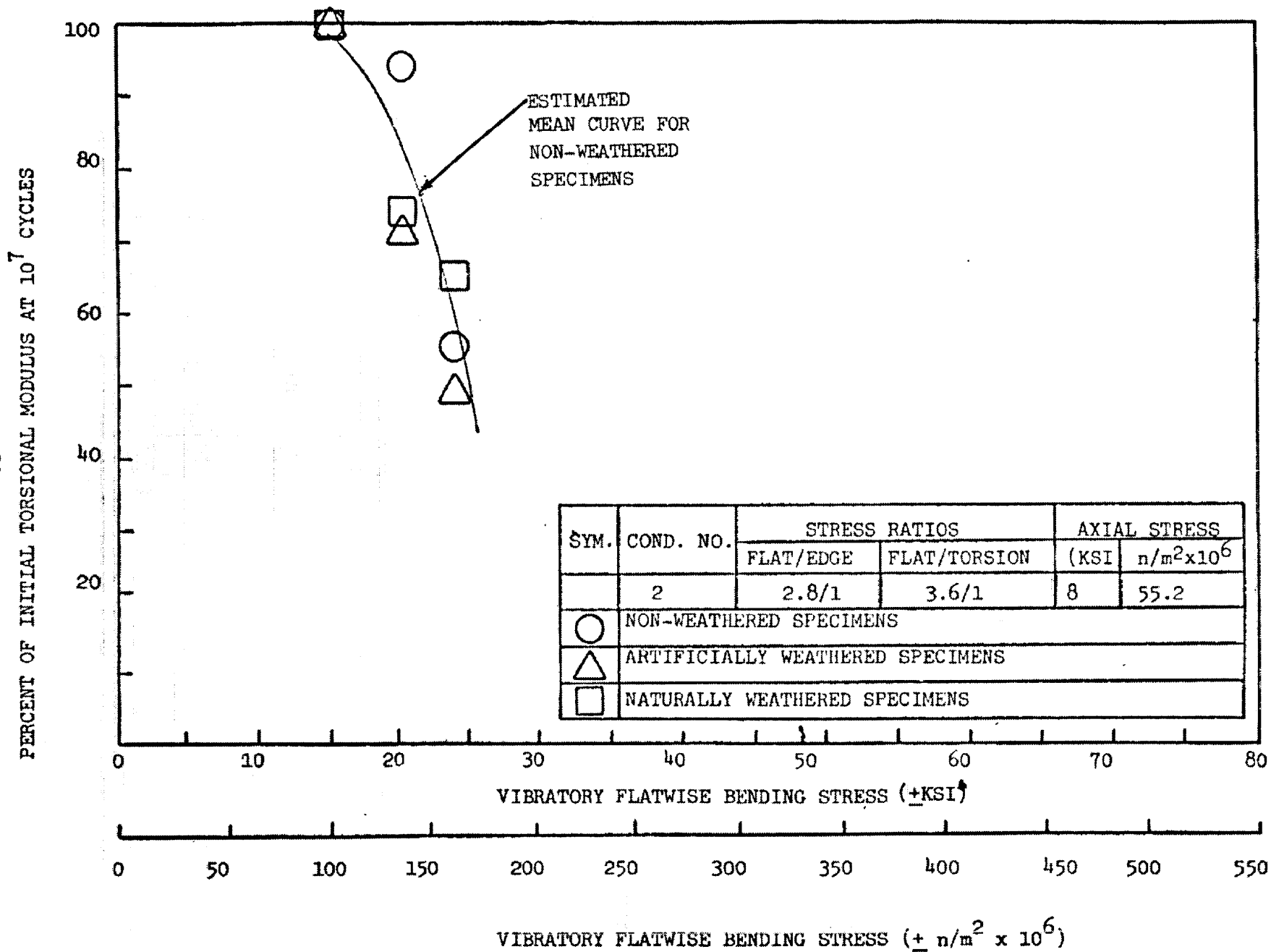


FIGURE 12b
WEATHERED VS. NON-WEATHERED FLATWISE BENDING TESTS RESULTS FOR CONDITION 2

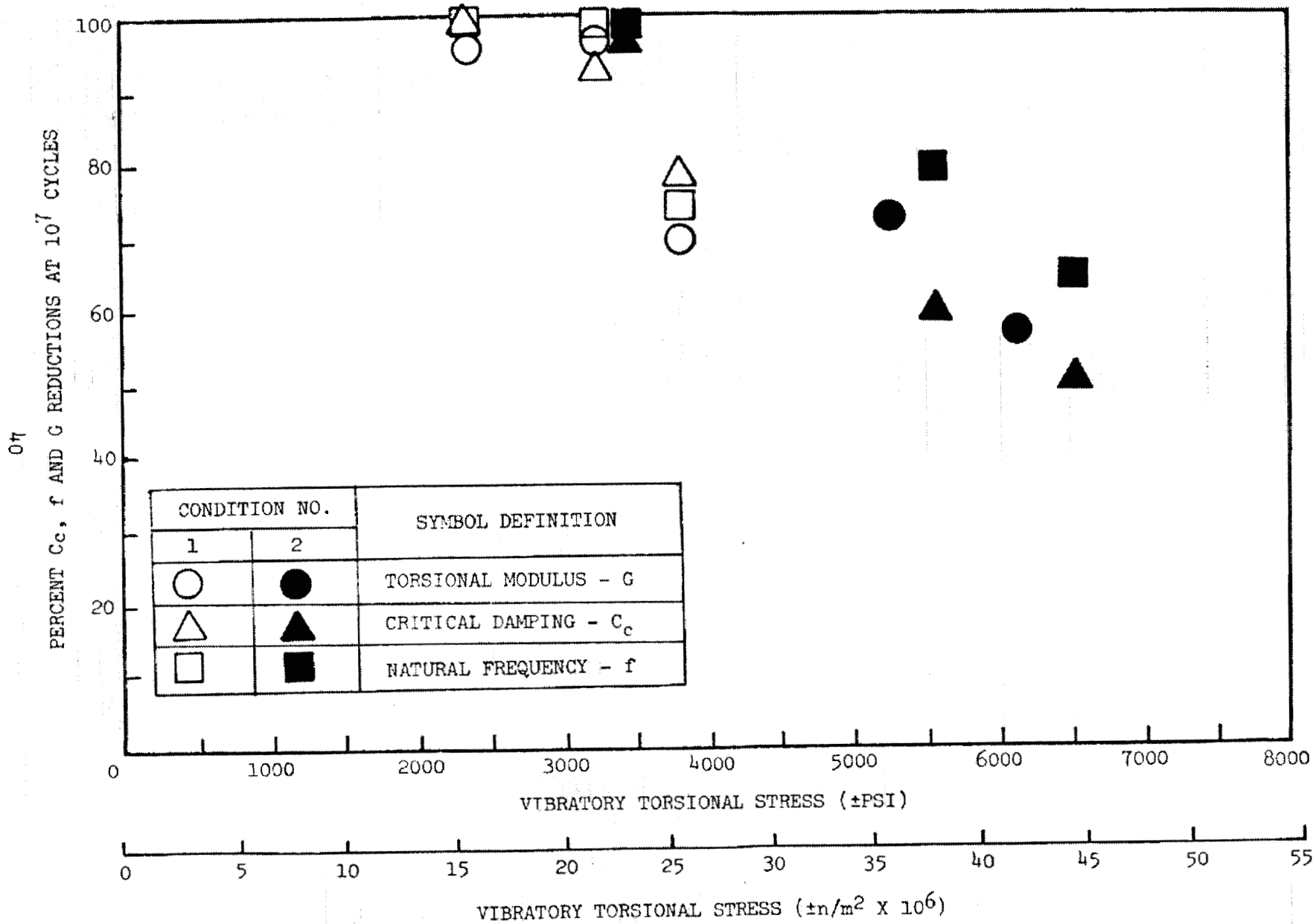


FIGURE 13

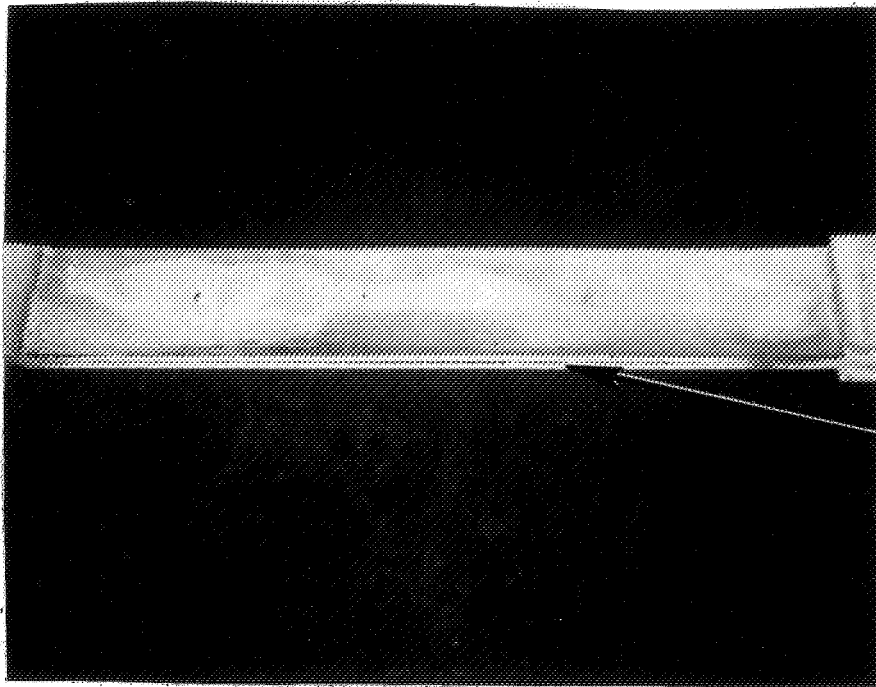


FIGURE (A)
TYPICAL
LONGITUDINAL
CRACKING
DAMAGE

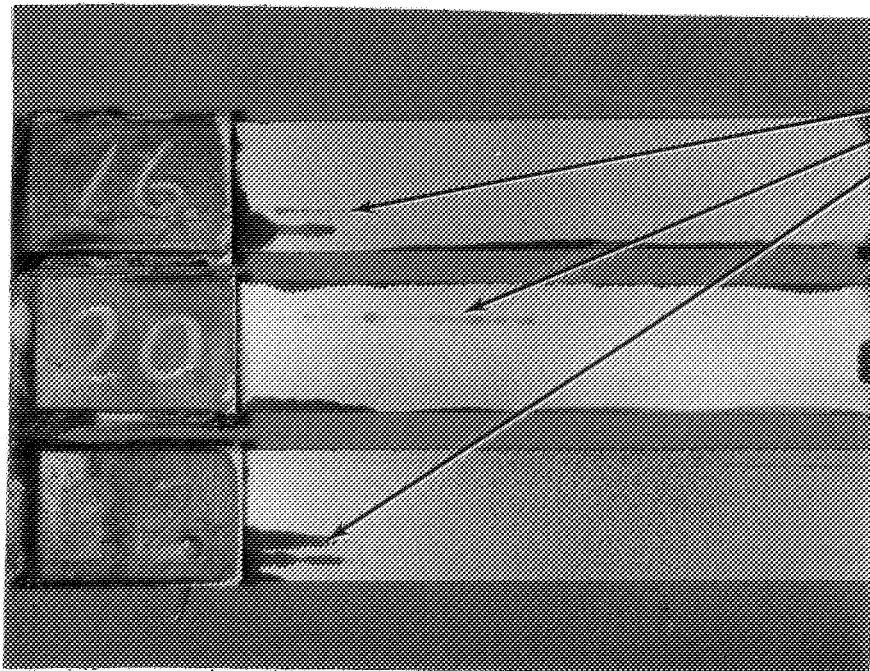
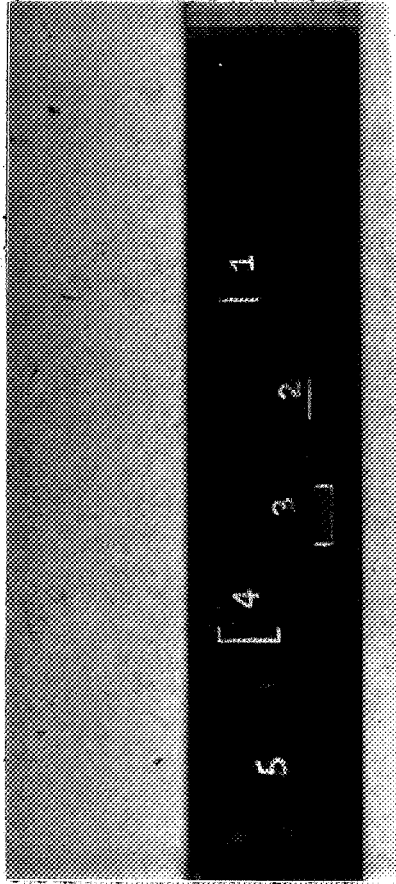


FIGURE (B)
TYPICAL VERTICAL
SURFACE CRACKS
VERIFIED BY
SECTIONED
PHOTO MICROGRAPH

FIGURE 14
DETECTION OF FATIGUE DAMAGE CRACKING BY DYE PENETRANT INSPECTION

SCAN 4
DIRECTION

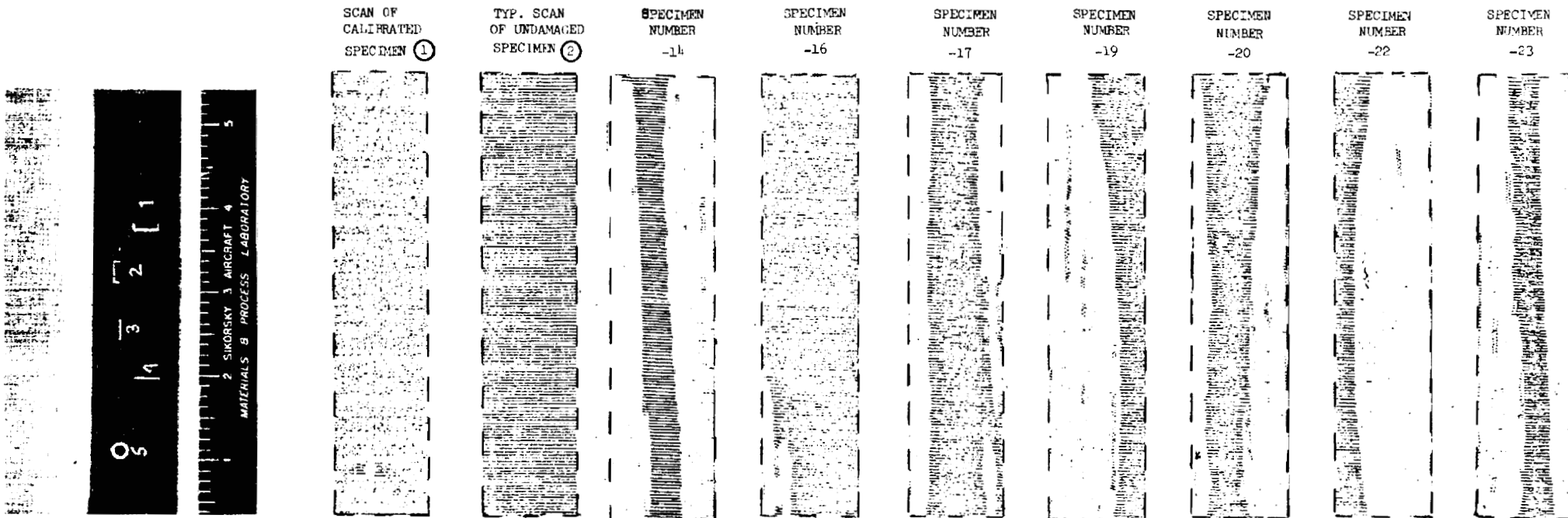
SCAN 1
DIRECTION



SCAN 2
DIRECTION

SCAN 3
DIRECTION

FIGURE 15
CALIBRATED SPECIMEN SHOWING THE FOUR SCANNING DIRECTIONS
TAKEN AT 20° ANGLE BEAM TO THE SPECIMEN



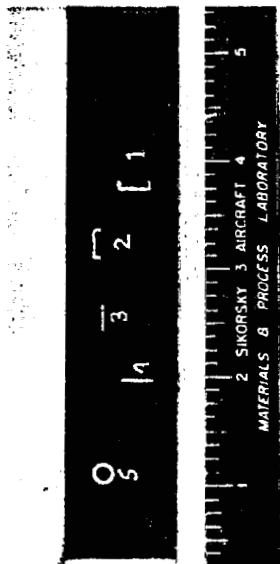
PERCENT OF DISBOND AREA	NOT MEASURED	NONE	69.0	5.0	35.0	64.0	52.0	75.0	64.0
PERCENT OF TORSIONAL MODULUS REDUCTION	NOT MEASURED	NONE	34.9	4.0	25.8	34.0	29.0	30.5	51.2

NOTES:

- ① WHITE AREA INDICATES DISBOND/DEFECT
- ② DASHED LINES SHOW SPECIMEN BOUNDARIES

FIGURE 16

ULTRASONIC STRAIGHT PULSE ECHO 'C' SCAN SHOWING PERCENT DISBOND AREA FOR EACH FATIGUE DAMAGED SPECIMEN



SCAN OF
CALIBRATED
SPECIMEN ①



TYP. SCAN
OF UNDAMAGED
SPECIMEN ②



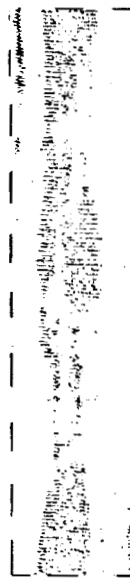
SPECIMEN
NUMBER
-14



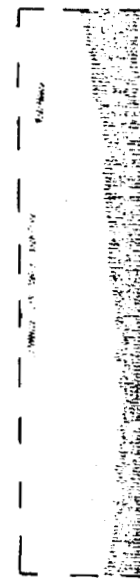
SPECIMEN
NUMBER
-16



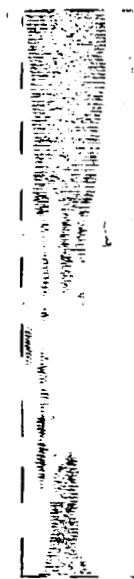
SPECIMEN
NUMBER
-17



SPECIMEN
NUMBER
-19



SPECIMEN
NUMBER
-20



SPECIMEN
NUMBER
-22



SPECIMEN
NUMBER
-23

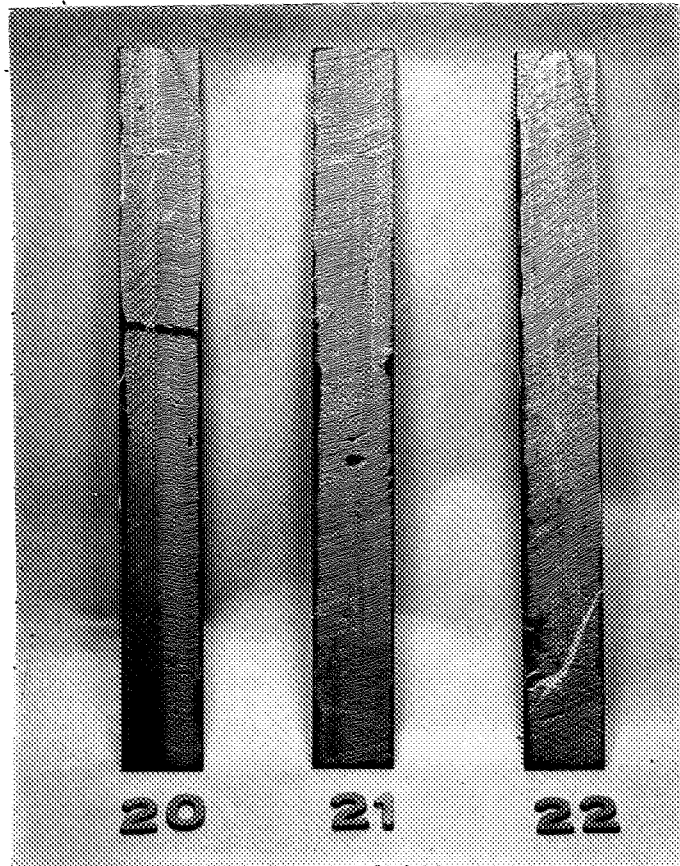


PERCENT OF DISBOND AREA	→ NOT MEASURED	NONE	77.0	29.0	58.0	66.0	58.5	59.0	71.0
PERCENT OF TORSIONAL MODULUS REDUCTION	→ NOT MEASURED	NONE	34.9	4.0	25.8	34.0	29.0	30.5	51.2

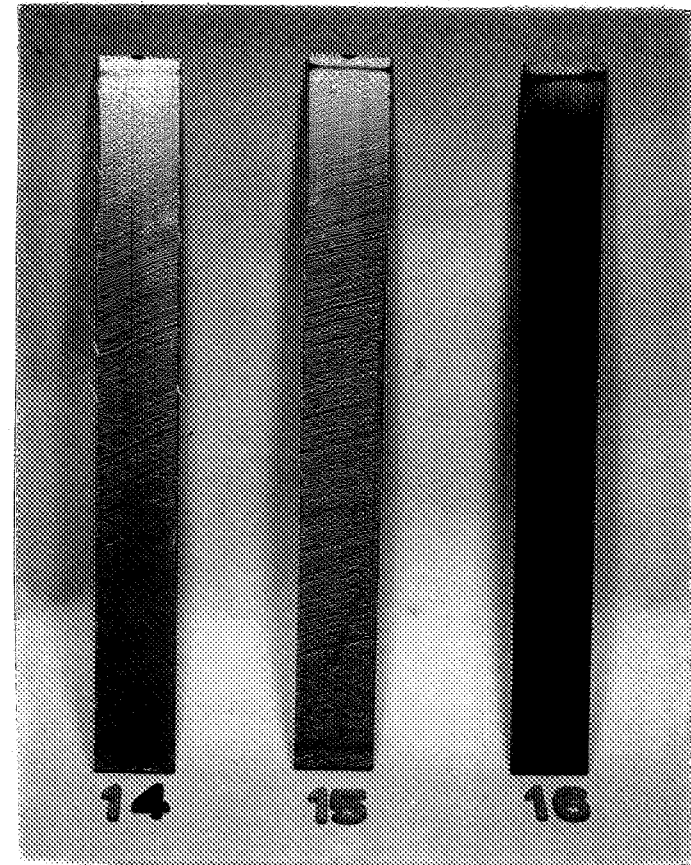
NOTES:

- ① WHITE AREA INDICATES DISBOND/DEFECT
- ② DASHED LINES SHOW SPECIMEN BOUNDARIES

FIGURE 17
ULTRASONIC LOSS OF BACK FACE 'C' SCAN SHOWING PERCENT DISBOND AREA FOR
EACH FATIGUE DAMAGED SPECIMEN



ARTIFICIALLY WEATHERED FOR 3 YEARS
TYPICAL SCRIM SIDE ONLY



NATURAL WEATHERED FOR 2 YEARS - TYPICAL
SCRIM VS. NON SCRIM SIDE EXPOSURE

FIGURE 18
TYPICAL ARTIFICIAL AND NATURAL WEATHERING EFFECTS SHOWING
SURFACE RESIN LEACH OUT EXPOSING SCRIM FIBERS.